THESIS

HEMOCOMPATIBILITY OF TITANIA NANOTUBE ARRAYS UNDER STATIC AND DYNAMIC CONDITIONS

Submitted by

Sayudh Ghosh

Department of Mechanical Engineering

In partial fulfilment of the requirements

For the Degree of Master of Science

Colorado State University

Fort Collins, Colorado

Fall 2020

Master's Committee:

Advisor: Ketul C. Popat

Zhijie Wang
Yan Li

ABSTRACT

HEMOCOMPATIBILITY OF TITANIA NANOTUBE ARRAYS UNDER STATIC AND DYNAMIC CONDITIONS

Titanium and titanium alloys have been extensively used to make blood contacting medical devices such as vascular stents, mechanical heart valves, etc. However, the material is not always hemocompatible, often resulting in thrombosis and eventual rejection of the medical device. To overcome this, medical practitioners have used anti coagulating methods which have had other detrimental effects on patients. Researchers have tried to overcome this problem by developing different surfaces for materials and evaluating hemocompatibility in static conditions, however it is important to evaluate hemocompatibility under dynamic conditions to get a realistic biological response. Recent studies have shown that nanotextured surfaces show better hemocompatibility than non-nanotextured surfaces. In this study, we have developed a dynamic chamber to evaluate hemocompatibility of titania nanotube arrays. The nanotube arrays were fabricated using anodization technique and modified to make the surface either supherhydrophobic or superhydrophillic. The stability of these surfaces and their interaction with blood and its components (protein adsorption, cell adhesion, platelet adhesion and activation) was investigated under dynamic flow conditions and compared to that from static conditions. The results indicate that the Titania nanotube arrays that were superhydrophobic show significantly enhanced hemocompatibility than other surfaces.

ACKNOWLEDGEMENTS

I would like to thank my advisor, Dr. Ketul Popat, first and foremost for providing me with this incredible opportunity to work under him for my Master's Thesis and for his continuous guidance and mentorship. Thank you for always being patient, caring and understanding throughout my graduate work.

I would like to show my respect and thank Dr. Patrick McCurdy from the chemistry department for training me on how to use the scanning electron microscope and the X-ray spectroscopy machine. These skills have been an integral part of my graduate degree and I am sure they will come of use further on in my career.

I would like to thank my colleagues in the lab: Roberta Sabino, Vignesh Manivasagam, Prem Kantam and Zach Montgomerie. Roberta showed me around the lab and trained me on multiple occasions over my first few months of my degree. She was always very patient and willing to help whenever I needed it. Vignesh, Prem and I started at the same time and both of them have helped me a lot throughout my graduate degree and it has always been a pleasure working alongside them. Zach was a wonderful guy to be around in the lab with impeccable work ethic. I wish all of you the best in life and I hope to see you all accomplish marvellous things in the future.

Finally, my deep and sincere gratitude to my family for their continuous support, help and unparalleled love. I am forever indebted to my parents, Surjendu Ghosh and Rakhi Ghosh for all the sacrifices they have made to provide me with the incredible experiences and opportunities that have made me who I am. None of this would have been possible without you.

TABLE OF CONTENTS

LIST OF TABLES

LIST OF FIGURES

INTRODUCTION

Cardiovascular disease is one of the most prevalent diseases in the whole world with one person dying in every 37 seconds and accounting for 23.4% of the total deaths in the United States(1). One of the common type of cardiovascular disease is coronary heart disease which is the blockage of the normal flow of blood to the heart where plaque is formed in the inner walls of the arteries that may lead to severe conditions like heart attack and stroke. Coronary heart disease is the most prevalent amongst the heart diseases killing 365,914 people in 2017(1). A treatment for coronary heart disease is a procedure called Angioplasty. In this procedure a stent is put inside the blood vessel at the site of the blockage to make sure that the blood can flow normally. However for many people, there are several short-term as well as long-term complications from the stent placement. Short-term complications include restenosis, which is the reoccurrence of the blockage inside the blood vessel due to denuding of endothelial cells followed by dedifferentiation of smooth muscle cells. Restenosis is commonly seen in bare metal stents(2,3). To resolve this problem, drug eluting stents(4) have been developed. Although the drug eluting stents prevent restenosis initially, the drug wears off after a certain time and the resulting bare metal stent that is left behind is again prone to late thrombosis. So for both types of stents, the material surface interaction with the tissue and the flowing blood is the main cause of failure (22.9% failure rate after 13 months (5)).

Whether it's a bare metal stent or a drug eluting stent, these will always be exposed to flowing blood, and thus it is very important to evaluate how blood and its components interact with the material surface under physiological conditions. Protein adsorption is the first phenomenon that takes place(6) followed by platelet adhesion and activation, and subsequent other processes that eventually lead to blood clot. The other components of blood like white blood cells and red blood cells also start adhering on the surface resulting in gradual increase in the size of clot. The clot not only can cause thrombosis(7) but if it is loosely attached on the surface, the flowing blood

can lift it off and transport it to the other parts of body causing stroke. These issues are not only restricted to stents but are applicable to any other medical device that may come in contact with the flowing blood, e.g. artificial heart valves, catheters, guide wires, etc. (8). For these reasons, it is not only critical to evaluate the interaction of foreign material surfaces with blood and its components under physiological flow conditions but also in static conditions. This will lead to better understanding of blood clotting process on material surface and further development of optimal material surface that can be used for blood contacting medical devices.

Titanium and titanium alloys (e.g. nitinol) have been extensively used to make blood contacting medical devices and implants(9–13) such as vascular stents, mechanical heart valves, etc. However, the surface of these materials is not always hemocompatible, often resulting in thrombosis(14) and eventual rejection of the medical device. To overcome this, medical practitioners have r\routinely used anti-coagulating therapies by administering drugs like heparin(15), warfarin(16), rivaroxaban(17) etc, to patients. However, these drugs have detrimental effects on patients, e.g. passing blood in their urine, nosebleeds, severe bruising, delay in blood clotting in case of an injury, etc. (18,19). Since thrombosis is a surface driven process, one of the best ways to prevent it is by engineering material surfaces that interact with blood and its components in a favorable way. Researchers have experimented by exposing blood and its components to material surfaces in static environments to understand different steps involved in whole blood clotting process such as protein adsorption, platelet adhesion and activation, coagulation, and thrombosis. Recent studies have shown that nanotextured surfaces show better hemocompatibility than non-nanotextured surfaces(20–22). Researchers have also found lower affinity towards blood components for materials surfaces that were modified with polymers that makes the surface either hydrophobic or hydrophilic. Most of these studies have been performed under static environments, however, it is also important to evaluate material surfaces under dynamic flow conditions. To bridge this gap, many researchers have developed a dynamic flow system. Parallel plate polycarbonate flow chambers with seeded endothelial

cells(23), single pass perfusion chambers(24), a pumped blood flow microchamber(25), modified Hele Shaw flow chamber(26) and chandler loops(27) are some of the examples of flow chambers that have been investigated.

In this study, titania nanotube arrays were fabricated using anodization process(28,29). Recent studies have shown that titania nanotube arrays show better hemocompatibility and reduced *in vitro* immune response than non-nanotextured surfaces(30,31) (21) (22). Studies have also shown that superhydrophobic surfaces show better hemocompatibility in general as the blood components tend to slide over the nanotubes without getting stuck or adhered to the surface thus preventing thrombosis and polymer coated surfaces tend to enhance this characteristic. Studies have previously shown that superhydrophobic surfaces have better hemocompatibiity(13,32,33), but most of these studies have been done in static conditions of blood. In this study, titania nanotube arrays were modified to have the surface either supherhydrophobic and superhydrophillic. Static studies were done by incubating these surfaces for two hours whereas for dynamic studies were done in a parallel plate flow chamber and fluid were appropriate fluid was flown at flow rates to mimic physiological conditions. The stability of these surfaces and their interaction with blood and its components (protein adsorption, cell adhesion, platelet adhesion and activation) was investigated under dynamic flow conditions and compared to that from static conditions. The results showed that there could be significant differences between static and dynamic processes depending on the things we are trying to measure.

HYPOTHESIS AND SPECIFIC AIMS

Fundamental Hypothesis: Both Static and Dynamic tests show similar trends of attachment for proteins and cells (platelets and leukocytes) although showing different results.

Hypothesis 1: Titania Nanotube surfaces can be modified to create superhydrophobic and superhydrophilic surfaces which are stable in both static and dynamic conditions.

Specific Aim 1: Fabrication and characterization of superhydrophilic, superhydrophobic and unmodified titania nanotube arrays. This specific aim is discussed in chapter 2 and will cover the following:

(a) Fabrication of uniformly distributed titania nanotube arrays by selective anodization.

(b) Fabrication of superhydrophobic and superhydrophilic surface coatings on the nanotube arrays.

(c) Characterization of titania nanotube surfaces using SEM and by measuring apparent water contact angles.

Hypothesis 2: Superhydrophobic titania nanotube arrays can reduce protein adsorption in both static and dynamic conditions.

Specific Aim 2: Characterization of protein adsorption on titania surfaces. This specific aim is discussed in chapter 3 and will cover:

(a) Exposure to human fibrinogen and human albumin and investigation of protein adsorption.

(b) Characterization of protein adsorption using BCA Assay and XPS.

Hypothesis 3: Superhydrophobic titania nanotube arrays can reduce cell adhesion in both static and dynamic conditions.

Specific Aim 3: Characterization of cell adsorption on titania surfaces. This specific aim is discussed in chapter 3 and will cover:

(a) Exposure to PRP and investigation of platelet, leukocyte adhesion and platelet activation.

(b) Characterization of cell adhesion using fluorescence microscopy and SEM.

REFERENCES

1. Heron M. National Vital Statistics Reports Volume 68, Number 6, June 24, 2019, Deaths: Leading Causes for 2017 [Internet]. 2019 [cited 2020 May 26]. Available from: https://www.cdc.gov/nchs/products/index.htm.

2. Bainey KR, Norris CM, Graham MM, Ghali WA, Knudtson ML, Welsh RC. Clinical in-stent restenosis with bare metal stents: Is it truly a benign phenomenon? International Journal of Cardiology [Internet]. 2008;128(3):378–82. Available from: http://www.sciencedirect.com/science/article/pii/S0167527307011102

3. Ovid: Abstract 10244: Drug Eluting Balloon - PCI is a New Therapeutic Option for Patients with In - Stent Restenosis in Bare Metal Stents. [Internet]. [cited 2020 Jun 19]. Available from: https://ovidsp-dc2-ovid-com.ezproxy2.library.colostate.edu/sp-4.06.0a/ovidweb.cgi?&S=OCBFFPMDBFEBBBGMJPBKPGHGGHLCAA00&Link+Set=S.sh.22%7c1%7csl_10&Counter5=SS_view_found_article%7c00003017-201111221-00107%7covft%7covftdb%7covftm&Counter5Data=00003017-201111221-00107%7covft%7covftdb%7covftm

4. Hao H, Ishibashi-Ueda H, Tsujimoto M, Ueda Y, Shite J, Gabbiani G, et al. Drug-Eluting Stent. Circulation Journal [Internet]. 2011 Jul [cited 2020 Jun 19];75(7):1548–58. Available from: http://joi.jlc.jst.go.jp/JST.JSTAGE/circj/CJ-11-0393?from=CrossRef

5. Heart Stent Surgery Safety - Heart Health - Everyday Health [Internet]. [cited 2020 May 27]. Available from: https://www.everydayhealth.com/heart-health/the-basics-on-heart-stent-surgery-safety.aspx

6. Xu LC, Bauer JW, Siedlecki CA. Proteins, platelets, and blood coagulation at biomaterial interfaces. Colloids and Surfaces B: Biointerfaces. 2014 Dec 1;124:49–68.

7. Xia S, Li J, Zu M, Li J, Liu J, Bai X, et al. Small size fullerenol nanoparticles inhibit thrombosis and blood coagulation through inhibiting activities of thrombin and FXa. Nanomedicine: Nanotechnology, Biology, and Medicine. 2018 Apr 1;14(3):929–39.

8. Jaffer IH, Fredenburgh JC, Hirsh J, Weitz JI. Medical device-induced thrombosis: What causes it and how can we prevent it? Vol. 13, Journal of Thrombosis and Haemostasis. Blackwell Publishing Ltd; 2015. p. S72–81.

9. Dobbs H. Titanium and its alloys for surgical implants: Phoenix, Arizona, USA, 11–12 May, 1981. Biomaterials [Internet]. 1981;2(4):250. Available from: http://www.sciencedirect.com/science/article/pii/0142961281900715

10. Gordin DM, Ion R, Vasilescu C, Drob SI, Cimpean A, Gloriant T. Potentiality of the "Gum Metal" titanium-based alloy for biomedical applications. Materials Science and Engineering: C [Internet]. 2014;44:362–70. Available from: http://www.sciencedirect.com/science/article/pii/S0928493114004883

11. Semlitsch M. Titanium alloys for hip joint replacements. Clinical Materials [Internet]. 1987;2(1):1–13. Available from: http://www.sciencedirect.com/science/article/pii/0267660587900151

12. Ghosh S, Abanteriba S, Wong S, Houshyar S. Selective laser melted titanium alloys for hip implant applications: Surface modification with new method of polymer grafting. Journal of the Mechanical Behavior of Biomedical Materials [Internet]. 2018;87:312–24. Available from: http://www.sciencedirect.com/science/article/pii/S1751616118308403

13. Li P, Li L, Wang W, Jin W, Liu X, Yeung KWK, et al. Enhanced corrosion resistance and hemocompatibility of biomedical NiTi alloy by atmospheric-pressure plasma polymerized fluorine-rich coating. Applied Surface Science [Internet]. 2014;297:109–15. Available from: http://www.sciencedirect.com/science/article/pii/S0169433214001329

14. Cayla G, Hulot JS, O'Connor SA, Pathak A, Scott SA, Gruel Y, et al. Clinical, angiographic, and genetic factors associated with early coronary stent thrombosis. JAMA - Journal of the American Medical Association [Internet]. 2011 Oct 26 [cited 2020 Jun 19];306(16):1765–74. Available from: https://jamanetwork-com.ezproxy2.library.colostate.edu/journals/jama/fullarticle/1104553

15. Comparison of high-dose with low-dose subcutaneous heparin to prevent left ventricular mural thrombosis in patients with acute transmural anterior myocardial infarction: Turpie AGG, Robinson JG, Doyle DJ, et al N Engl J Med 320:352–357, 1989. Journal of Cardiothoracic Anesthesia [Internet]. 1989;3(5):665. Available from: http://www.sciencedirect.com/science/article/pii/088862968990183X

16. Do EJ, Lenzini P, Eby CS, Bass AR, McMillin GA, Stevens SM, et al. Genetics informatics trial (GIFT) of warfarin to prevent deep vein thrombosis (DVT): Rationale and study design. Pharmacogenomics Journal [Internet]. 2012 Oct 24 [cited 2020 Jun 19];12(5):417–24. Available from: https://www.nature.com/articles/tpj201118

17. Kaeberich A, Reindl I, Raaz U, Maegdefessel L, Vogt A, Linde T, et al. Comparison of unfractionated heparin, low-molecular-weight heparin, low-dose and high-dose rivaroxaban in preventing thrombus formation on mechanical heart valves: Results of an in vitro study. Journal of Thrombosis and Thrombolysis [Internet]. 2011 Nov 20 [cited 2020 Jun 19];32(4):417–25. Available from: https://link-springer-com.ezproxy2.library.colostate.edu/article/10.1007/s11239-011-0621-6

18. Fiumara K, Goldhaber SZ. Cardiology patient pages. A patient's guide to taking coumadin/warfarin. Circulation [Internet]. 2009 Mar 3 [cited 2020 Jun 19];119(8):e220-2. Available from: http://www.ncbi.nlm.nih.gov/pubmed/19255348

19. Anticoagulant Medicine: Potential for Drug-Food Interactions [Internet]. [cited 2020 Jun 19]. Available from: https://www.nationaljewish.org/conditions/medications/cardiology/anticoagulant-and-drug-food-interactions

20. Bartlet K, Movafaghi S, Kota A, Popat KC. Superhemophobic titania nanotube array surfaces for blood contacting medical devices. RSC Advances. 2017 Jul 17;7(56):35466–76.

21. Smith BS, Capellato P, Kelley S, Gonzalez-Juarrero M, Popat KC. Reduced in vitro immune response on titania nanotube arrays compared to titanium surface. Biomaterials Science. 2013 Mar 4;1(3):322–32.

22. Smith BS, Yoriya S, Grissom L, Grimes CA, Popat KC. Hemocompatibility of titania nanotube arrays. Journal of Biomedical Materials Research - Part A. 2010 Nov;95 A(2):350–60.

23. Otto M, Franzen A, Hansen T, Kirkpatrick CJ. Modification of human platelet adhesion on biomaterial surfaces by protein preadsorption under static and flow conditions. Journal of Materials Science: Materials in Medicine. 2004 Jan;15(1):35–42.

24. Saelman EU, Nieuwenhuis HK, Hese KM, de Groot PG, Heijnen HF, Sage EH, et al. Platelet adhesion to collagen types I through VIII under conditions of stasis and flow is mediated by GPIa/IIa (α2β1-integrin). Blood [Internet]. 1994;83(5):1244–50. Available from: http://www.ncbi.nlm.nih.gov/pubmed/8118028

25. Liu L, Koo Y, Collins B, Xu Z, Sankar J, Yun Y. Biodegradability and platelets adhesion assessment of magnesium-based alloys using a microfluidic system. PLoS ONE. 2017 Aug 1;12(8).

26. Goto S, Ikeda Y, Saldívar E, Ruggeri ZM. Distinct mechanisms of platelet aggregation as a consequence of different shearing flow conditions. Journal of Clinical Investigation. 1998 Jan 15;101(2):479–86.

27. Slee JB, Alferiev IS, Levy RJ, Stachelek SJ. The use of the Ex Vivo Chandler Loop Apparatus to assess the biocompatibility of modified polymeric blood conduits. Journal of Visualized Experiments. 2014 Aug 20;(90).

28. Paulose M, Prakasam HE, Varghese OK, Peng L, Popat KC, Mor GK, et al. TiO 2 nanotube arrays of 1000 μm length by anodization of titanium foil: Phenol red diffusion. Journal of Physical Chemistry C [Internet]. 2007 Oct 18 [cited 2020 Jun 22];111(41):14992–7. Available from: https://pubs.acs.org/doi/abs/10.1021/jp075258r

29. Popat KC, Eltgroth M, LaTempa TJ, Grimes CA, Desai TA. Titania nanotubes: A novel platform for drug-eluting coatings for medical implants? Small [Internet]. 2007 Nov 5 [cited 2020 Jun 22];3(11):1878–81. Available from: https://onlinelibrary.wiley.com/doi/full/10.1002/smll.200700412

30. Smith BS, Capellato P, Kelley S, Gonzalez-Juarrero M, Popat KC. Reduced in vitro immune response on titania nanotube arrays compared to titanium surface. Biomaterials Science. 2013 Mar 4;1(3):322–32.

31. Smith BS, Yoriya S, Johnson T, Popat KC. Dermal fibroblast and epidermal keratinocyte functionality on titania nanotube arrays. Acta Biomaterialia. 2011 Jun;7(6):2686–96.

32. Ye X, Wang Z, Zhang X, Zhou M, Cai L. Hemocompatibility research on the micro-structure surface of a bionic heart valve. In: Bio-Medical Materials and Engineering. IOS Press; 2014. p. 2361–9.

33. Huang Q, Yang Y, Hu R, Lin C, Sun L, Vogler EA. Reduced platelet adhesion and improved corrosion resistance of superhydrophobic TiO2-nanotube-coated 316L stainless steel. Colloids and Surfaces B: Biointerfaces [Internet]. 2015;125:134–41. Available from: http://www.sciencedirect.com/science/article/pii/S0927776514006511

Chapter 1

LITERATURE REVIEW

1.1 Introduction

Titanium and titanium alloys have been extensively used to make blood contacting medical devices such as vascular stents, mechanical heart valves, etc. However, the material is not always hemocompatible, often resulting in thrombosis and eventual rejection of the medical device. To overcome this, medical practitioners have used anti coagulating methods which have had other detrimental effects on patients. Researchers have tried to overcome this problem by developing different surfaces for biomaterials and evaluating hemocompatibility in static conditions, however it is important to evaluate hemocompatibility under dynamic conditions to get a realistic biological response for the entire body. Recent studies have shown that nanotextured surfaces show better hemocompatibility than non-nanotextured surfaces. Since hemocompatibility is a surface driven process, in this study we have developed a dynamic chamber to evaluate hemocompatibility of titania nanotube array surfaces along with further modifications. The nanotube arrays were fabricated using anodization technique and modified to make the surface either supherhydrophobic or superhydrophillic. The stability of these surfaces was investigated in both static and dynamic conditions by exposing them to Hepes-tyrode solution. Their interaction with blood and its components (protein adsorption, cell adhesion, platelet adhesion and activation) was investigated under dynamic flow conditions and compared to the results from static conditions. The results indicate that the titania nanotube arrays that were superhydrophobic show significantly enhanced hemocompatibility than other surfaces. Thus, further investigation on these materials might be a promising approach to preventing thrombogenic reactions to blood contacting implants.

1.2 Cardiovascular implants and other blood contacting devices

Cardiovascular disease is one of the most prevalent diseases in the whole world with one person dying in every 37 seconds and accounting for 23.4% of the total deaths in the United States(1). Heart Disease remains the number 1 cause of death in the US. Coronary heart disease accounted for approximately 13% of deaths in the US in 2017, causing 365,914 deaths. According to data from 2005 to 2014, the estimated annual incidence of heart attack in the US was 605,000 new attacks and 200,000 recurrent attacks(2,3). Prevalence of cardiovascular diseases in the US of ages 20 years or older is documented as below.

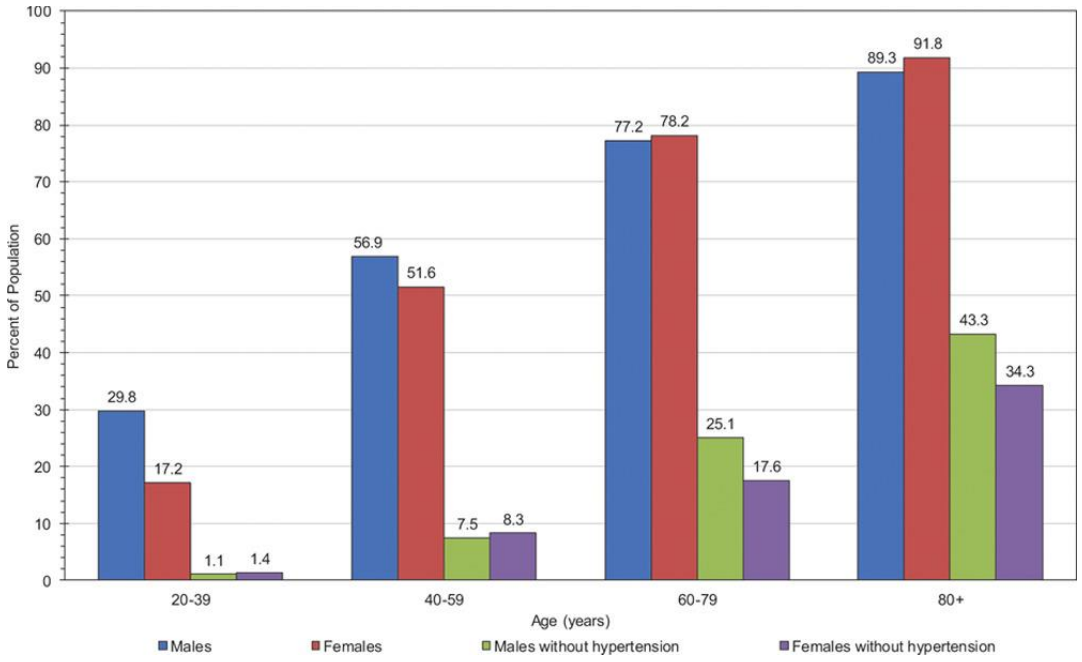

Fig 1.2.1 The above data includes coronary heart disease, heart failure, stroke, and with and without hypertension(4).

One of the common type of cardiovascular disease is coronary heart disease, which is the blockage of the normal flow of blood to the heart where plaque is formed in the inner walls of the arteries that may lead to severe conditions like heart attack and stroke. The leading cause of coronary heart disease is the gradual deposition of plaque, cholesterol, fat on the inner lining of

coronary arteries. The depositions can build up to partially or completely block the flow of blood. Another example of a coronary heart disease is the coronary microvascular disease where the smaller blood vessels of the heart are not able to work normally (3). A preferred procedure of treatment for coronary heart disease is angioplasty where a stent is inserted into the artery at the site of the blockage to keep the blood flowing normally. This leads to many further complications like restenosis, which is the reoccurrence of the blockage inside the blood vessel due to denuding of endothelial cells followed by dedifferentiation of smooth muscle cells. Restenosis is commonly seen in bare metal stents(5,6)(7). To resolve this problem, drug eluting stents have been developed(7). Although the drug eluting stents prevent restenosis initially, the drug wears off after a certain time and the resulting bare metal stent that is left behind is again prone to late thrombosis. In the pre-stent era the occurrence of restenosis ranged between 32–55% of all angioplasties, and drop to successively 17–41% in the bare metal stents (BMS) era. The advent of drug-eluting stent (DES), especially 2nd generation, and drug-coated balloon (DCB) further reduce restenosis rate until <10% (understanding and managing). So, for both types of stents, the material surface interaction with the tissue and the flowing blood is the main cause of failure (22.9% failure rate after 13 months)(8).

Fig 1.2.2: Design representation of a cardiovascular stent. Reprinted with permission from Elsevier: Saraf AR, Yadav SP. Fundamentals of bare-metal stents. In: Functionalised Cardiovascular Stents. Elsevier; 2018. p. 27–44. Copyright (2018) (9).

Another common artificial cardiac device used is an artificial heart valve. Artificial heart valves are used to replace a heart valve that is dysfunctional. Heart valves operate in synchrony with every heartbeat to maintain normal blood flow inside the human body. Sometimes due to improper health conditions, heart valves can leak or completely stop working resulting in severe heart malfunction. In cases where the heart valve cannot be repaired, an open heart surgery procedure is done where the valve is replaced by an artifial heart valve known as heart valve replacement. Artificial heart valves are mainly of two types: mechanical valves and biological valves. Mechanical heart valves (MHVs) are generally more prone to thrombosis than biosynthetic heart valves (BHVs), which are developed from bovine or porcine tissue mounted on a metal frame(10). But, in general MHVs last longer than BHVs although consumption of blood thinners are necessary in case of MHVs.

Fig 1.2.3: Image of a mechanical heart valve (MHV). Reprinted with permission from Wolters Kluwer Health, Inc.: Dangas GD, Weitz JI, Giustino G, Makkar R, Mehran R. Prosthetic Heart Valve Thrombosis [Internet]. Vol. 68, Journal of the American College of Cardiology. Elsevier USA; 2016 [cited 2020 Oct 7]. p. 2670–89. Available from: https://pubmed.ncbi.nlm.nih.gov/27978952/; Copyright (2009) (10).

Guide wires are also blood contacting devices used with catheters which are susceptible to thrombus formation. Significant thrombus formation on angioplasty guide wires was a frequent finding, occurring in 48% of cases(11). Catheters and guide wires interact with blood resulting in thromboembolic complications occurring during angiography(12). Infections associated with guide wires can be deadly to the patients as it can lead to thrombosis. In the case of thrombus formation or even with infection growth, the guide wires and the catheters need replacement which exposes the patient to serious health risks. Thrombus formation on an indwelling catheter might be a cause of a lot of factors like the size of the catheter compared to the surrounding vein or the artery and most importantly the biocompatibility of the catheter and the guide wire with the cellular environment to avoid cell aggregation and eventual thrombus formation (13,14). To avoid infections or thrombus formation catheters and guide wires have been modified by coating them with heparin to make them biocompatible. Research shows that Many efforts have been made to limit thrombosis on guide wires or catheters by coating them with heparin. show that 90/10 Na-hep provides a coating with a high degree of thrombus resistance. Sodium heparin is released from the catheter and guide wire surface to assist with the safe diagnostic and therapeutic interventional treatments (11).

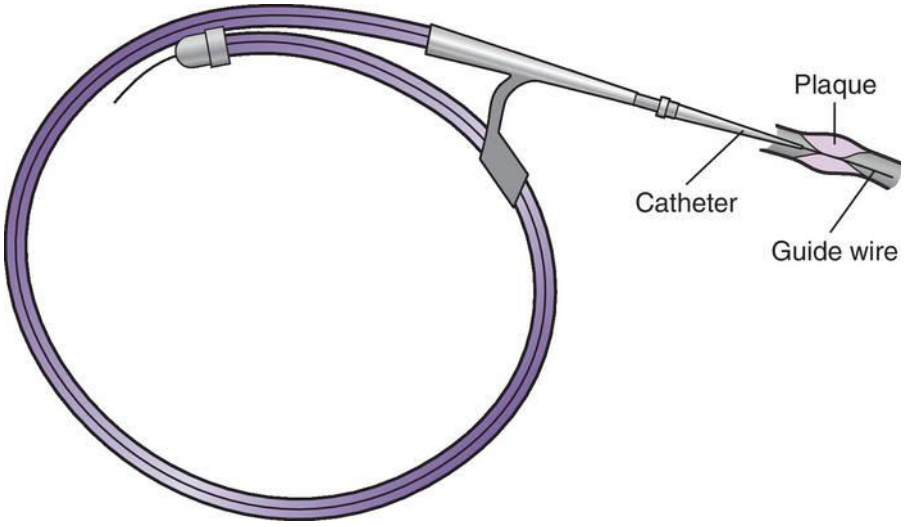

Fig 1.2.4: Representation of a Guide Wire. Reprinted from Farlex Partner Medical Dictionary: Guidewire | definition of guidewire by Medical dictionary [Internet]. [cited 2020 Oct 16]. Available from: https://medical-dictionary.thefreedictionary.com/guidewire (15).

In all of these cases, the blood contacting devices are either susceptible to thrombus formation and eventual failure and a way around this inevitability is the usage of blood thinners like heparin which leads to numerous other complications. Thus, it is very important to research on the possibilities of increasing the hemocompatibility of the blood contacting medical devices to improve the functional life of these devices.

1.3 Titanium and titanium alloys as implant material

Titanium and titanium alloys (e.g. nitinol) have been extensively used to make blood contacting medical devices and implants such as vascular stents, mechanical heart valves, etc (16–20). Titanium has a very high corrosion resistance coupled and its light weight makes it ideal as an implant material. Titanium and titanium alloys were always preferred as biomaterials due to certain physical qualities like increased biocompatibility, low density and corrosion resistance.some of the popular biomaterials used are CP-Ti and an alloy of Ti, Ti–4Al–6V (grade 5 ELI)(17). Ti-6Al-4V, made of titanium, aluminum, and vanadium, is the most commonly used alloy in prosthetic devices. Along with their biocompatibility, these materials are also compliant with the different medical imaging technologies used like CT (computed tomography) scanning and MRI (magnetic resonance imaging). Ti alloys with Ta, Fe, Zr, Nb along with TiMo show better mechanical properties like improved toughness, formability and lower modulus(21). Another titanium alloy is Nickel-titanium alloy Nitinol. Nitinol is widely used as a stent material as it has a better biocompatibility than most other metals along with its superelastic properties. Nitinol has an elastic modulus close to the human bone which makes it an appealing implant material(21). Although Ti and its alloys performed better over other metals as implant material, there are still concerns over its long term compatibility as blood contacting surfaces due to its tendency to

induce thrombus formation over a period of time. Titanium alloys like NiTi can also be hazardous due to its release of toxic Ni into the blood stream and the ensuing inflammatory reactions. Thus, it is necessary to research on surface modifications on titanium to make it more biocompatible without the addition of other potential toxic substances like Ni.

To avoid the adverse effects of alloys and improve the hemocompatibility of titanium surfaces, proposed methods include heparin-based surface coatings, diamond-like carbon surfaces, modified surface coatings, and titania nanostructures(22). Heparin coated surfaces has been widely used as blood contacting devices, especially stents and guide wires(23–26). By limiting the formation of thrombin, heparin improves the hemocompatibility of the surfaces(24,27). The downside of heparin usage is it is still a blood thinner and can cause other detrimental effects. Other surface modifications include coating with carbon films because of its inherent inert nature. But, the downside for diamond-like carbon surfaces is its manufacturability and expense.

Another method used to improve hemocompatibility is by making the titanium surfaces superhemophobic(22). To create superhemophobic surfaces, both the surface topography and chemistry was modified. Previous studies indicated that creation of titania nanostructures showed enhanced hemocompatibility(22,28,29). The surface topography was altered by creating nanostructures, like nanopores, nanotubes and nanoflowers. The modified surfaces were then coated with silanes either in vapor phase or in liquid phase to attain a uniform coating. The result of these modifications were the creation of titanium surfaces that were superhemophobic. In this study some of these modifications were applied and their stability on different flow conditions were tested.

1.4 Surface modifications at a nano-scale on titanium

Recent studies have shown that nanotextured titanium surfaces show better hemocompatibility than non-nanotextured surfaces(28,30,31). Nano-textures on the surface of titanium improves its integration to various cellular environments. The three major approaches of

constructing nanostructures on titanium are template-assisted, electrochemical and hydrothermal methods(32). In the template-assisted process of nanotube formation, controlling a sol-gel hydrolysis of a titanium precursor is used to prepare TiO2. The template morphology is then reproduced by allowing the TiO2 to deposit on the template. The deposition of TiO2 can be altered by using either a positive or a negative template. In case of a positive template, TiO2 is allowed to deposit on the outside whereas in case of a negative template TiO2 is allowed to deposit inside the template. Prior to annealing (heat treatment at 500 C) the templates are removed by a chemical based solvent to form titania nanostructures.

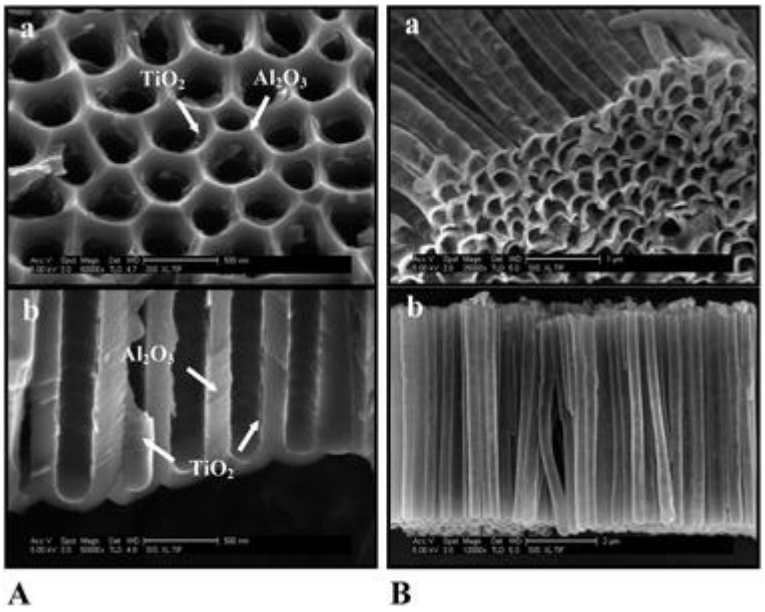

Fig 1.4.1: (A) Alumina template SEM images following infiltration and heat treatment at 500 °C for 30 mins. (a) top-down view and (b) crossectional view. (B) SEM images of TiO2 nanotube arrays following the removal of the alumina template. a) top-down view and (b) cross-sectional view. Reprinted with permission of Royal Society of Chemistry, from Damodaran VB, Bhatnagar D, Leszczak V, Popat KC. Titania nanostructures: A biomedical perspective [Internet]. Vol. 5, RSC Advances. Royal Society of Chemistry; 2015 [cited 2020 Oct 3]. p. 37149–71. Available from: www.rsc.org/advances(32) ; Copyright The Royal Society of Chemistry 2015; permission conveyed through Copyright Clearance Center, Inc.

A very common method of preparing nanostructures is by electrochemical anodization in which two electrodes are used to perform anodization. Titanium is used as an anode and the platinum is used as cathode in the presence of an electrolyte containing fluoride-ion. The

electrolytic solution for the anodization contains hydrofluoric acid which erodes the surface to form nanotubes. Selective etching on the surface of Ti (eqn i) resulted in pits followed by chemical dissolution which resulted in the nanopores (eqn ii). These nanopores were allowed to grow for 22 hours to attain tubular geometries thus resulting in nanotubes on the surface.(33).

$$Ti + 2H_2O \rightarrow TiO_2 + 4H^+ + 4e^- \qquad (i)$$

$$TiO_2 + 6F^- + 4H^+ \rightarrow [TiF_6]^{2-} + 2H_2O \qquad (ii)$$

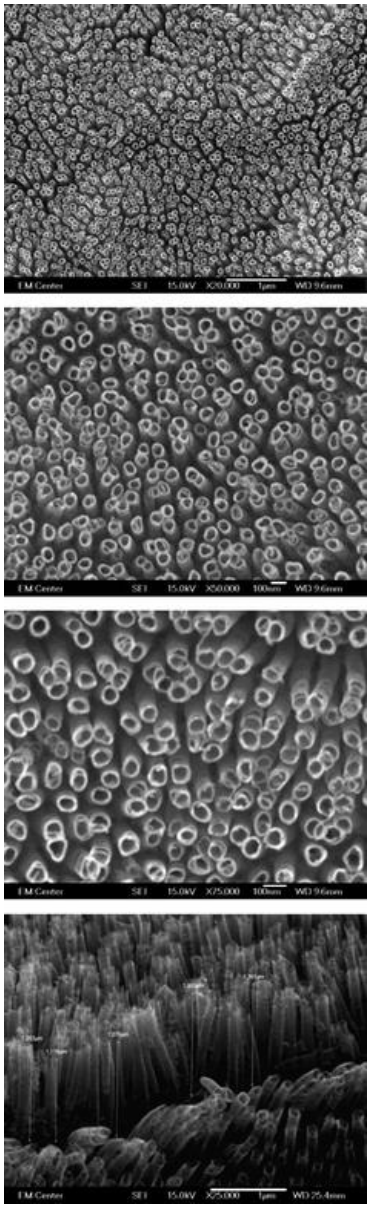

Fig 1.4.2: Representative titania nanotube arrays at different magnifications (20 000×, 50 000×, 75 000×) and height of titania nanotubes prepared by electrochemical anodization. Reprinted with permission of Royal Society of Chemistry, from Damodaran VB, Bhatnagar D, Leszczak V, Popat KC. Titania nanostructures: A biomedical perspective [Internet]. Vol. 5, RSC Advances. Royal Society of Chemistry; 2015 [cited 2020 Oct 3]. p. 37149–71. Available from: www.rsc.org/advances(32) ; Copyright The Royal Society of Chemistry 2015; permission conveyed through Copyright Clearance Center, Inc.(34)

The size and diameter of the titanium nanotubes can be modified by adjusting the applied voltage, electrolyte composition, pH level and anodizing time(35–37). The hydrothermal method of preparing nanotubes includes treatment with NaOH, hydrochloric acid which results in a reduction of the distance between the atoms of Ti on the surface which results in eventual formation of tubular geometries. Surfaces with anodized TiO2 nanotube modification have shown an enhanced biocompatibility by creating a better atmosphere for the cells and by mimicking the inner walls of the arteries which results in better endothelial cell growth and improving ECM deposition in comparison to an unmodified Ti surface(37). The ratio of release of nitric oxide over endothelin-1 is also improved by TiO2 nanotube surfaces whin in turn helps in reduction of platelet activation and aggregation and regulation of the factors influencing thrombosis(32).

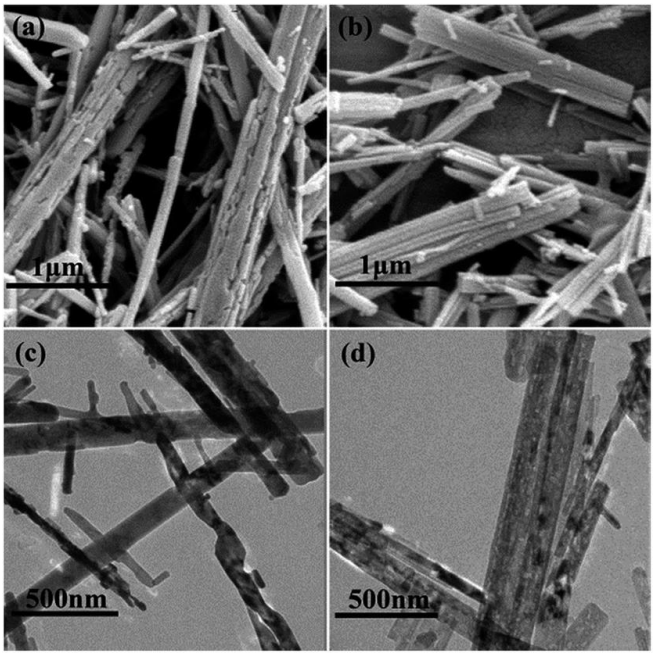

Fig 1.4.3: (a) & (b) SEM images of titania nanobelt formation with and without ethanol treatment. (c) & (d) TEM images of the same. Reprinted with permission of Royal Society of Chemistry, from Damodaran VB, Bhatnagar D, Leszczak V, Popat KC. Titania nanostructures: A biomedical perspective [Internet]. Vol. 5, RSC Advances. Royal Society of Chemistry; 2015 [cited 2020 Oct 3]. p. 37149–71. Available from: www.rsc.org/advances(38) ; Copyright The Royal Society of Chemistry 2015; permission conveyed through Copyright Clearance Center, Inc.

1.5 Interaction of material surfaces with blood and its components – protein adsorption, cell adhesion, thrombus formation.

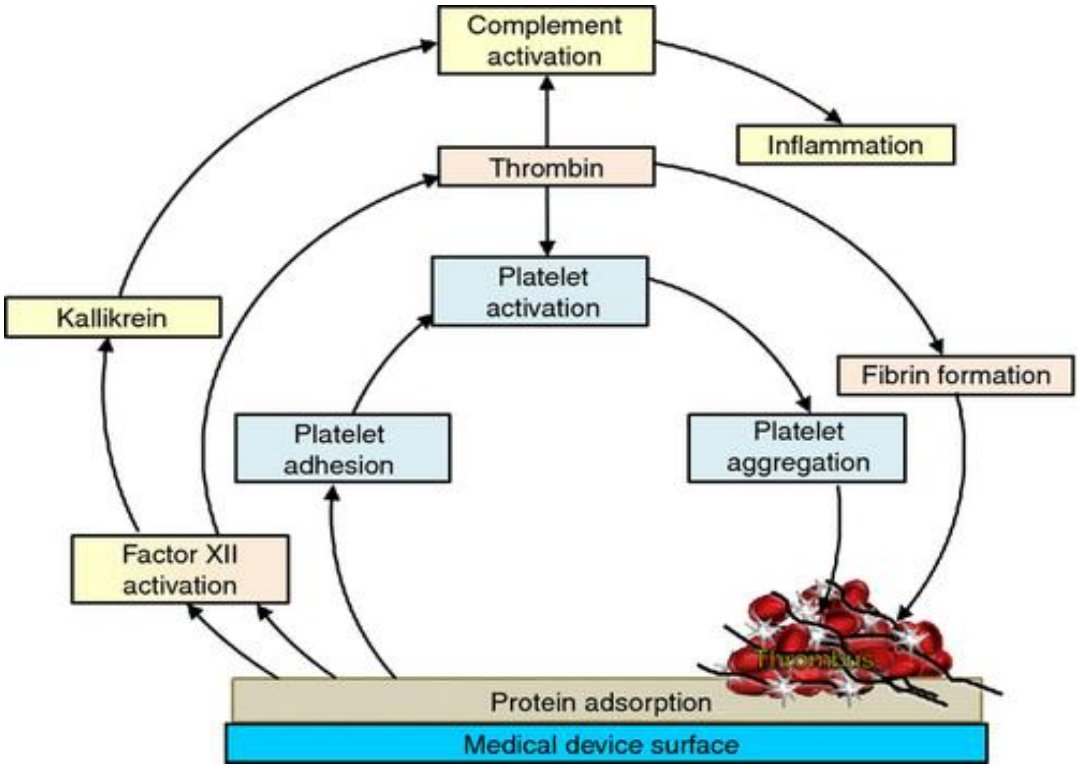

Fig 1.5.1: Figure represents medical device induced protein adsorption that initiates thrombin formation. Protein adsorption induces platelet adhesion, platelet activation and platelet aggregation. Auto-activation of Factor XII induces the formation of Kallilrein which leads to thrombin formation. Thrombin not only forms fibrin, it also induces platelet activation. Fibrin acts as a stabilizer for the deposited platelet aggregates and fibrin, platelet aggregates and inflammation together leads to thrombus formation. Reprinted with permission from John Wiley and Sons: Jaffer IH, Fredenburgh JC, Hirsh J, Weitz JI. Medical device-induced thrombosis: What causes it and how can we prevent it? [Internet]. Vol. 13, Journal of Thrombosis and Haemostasis. Blackwell Publishing Ltd; 2015 [cited 2020 Sep 27]. p. S72–81. Available from: https://onlinelibrary.wiley.com/doi/full/10.1111/jth.12961: Copyright 2015 International Society on Thrombosis and Haemostasis. License at http://creativecommons.org/licenses/by/3.0/ (39).

Contact activation is observed when blood components and plasma come in contact to non-endothelial surfaces(39). Blood contact with synthetic surfaces initiates plasma protein adsorption and activates platelets and Factor XII which initiates the clotting cascade. Thus it is particularly important to study protein adsorption and cell adhesion on different surfaces. Fibrinogen and albumin are all adsorbed on the surfaces and the amount of adsorption depends on the surface material it is exposed to(40–42). After water and ions are absorbed on the foreign surface, the first event that follows is protein adsorption(40–46). The interaction of cells with the materials is driven by the nature of the absorbed proteins which act as the mediator between the material and the cell receptors thus becoming an integral reason for the success or failure of the implant(39).

Platelet adhesion is followed by activation of platelets which leads to an inflammatory response in the whole body(46). Initial stages of cell interaction is solely dependant on the surface properties since the nature of adsorbed proteins depend entirely on the surface characteristics which lead to cell reception whereas in the longer term, cell interaction is mostly related to the formation of extra-cellular matrix and alteration of the surface (11). Proteins are attracted to surfaces with higher surface energy and with higher adhesion of proteins, cell adhesion also increases due to the presence of proteins like fibrinogen on the surface. Another reason for higher protein adsorption on higher charged (hydrophilic) surfaces is the better biocompatibility of the surfaces which makes it prone to protein denaturation.

Thrombosis is one of the leading factors for the failure of blood contacting implants. The presence of thromboregulators like nitric oxide, prostacyclin and the ectonucleotidase CD39 in the endothelium provides a defence mechanism against the formation of thrombosis. In case of blood contacting implants, when the vessel wall is breached or the endothelial layer is disrupted, collagen and tissue factors are exposed to the flowing blood which leads to thrombin formation(39). In the presence of external materials induces contact activation of the platelets when exposed to blood and its components. Contact activation is caused when blood components

come in contact with external or non-endothelial surfaces. A blood comes in contact with a synthetic material, plasma proteins like fibrinogen albumin immunoglobulin, hemoglobin are all absorbed onto the surface. Proteins like Fibrinogen are responsible for the initiation of the clotting cascade for blood which starts by absorbing activated platelets onto the surface(39). Another initiating factor is the presence of Factor XII. In the presence of kallikrein, surface bound Factor XII activates formin Factor XIIa and Factor XIIf. This in turn produces bradykinin and also initiates the clotting cascade. In the presence of Factor XIIa and kallikrein another primary contact protein Factor XI ids activated which initiates the coagulation process and the formation of thrombin, which converts the fibrinogen into fibrin(47). FXIIa is cleaved by Kallikrein which further activates the C1q complex protein(39). FXIIa also activates the complement system and generates the anaphylactoxins C3a and C5a via the classical pathway(47). Activated C3 and C5 further promote the adhesion and activation of leukocytes on to the artificial surfaces(48). Thrombin cleaves protease-activated receptor 4 on the platelet surface resulting in platelet activation(11). This in turn amplifies thrombus formation by activating platelets with the release of agonising agents like thromboxane A_2, adenosine diphosphate (ADP) and serotonin(49). In easier terms, protein adsorption on the surfaces initiates the formation of thrombosis. Protein adsorption is followed by plated activation and adhesion on the surfaces although the exact reason for the activation of platelets is unknown and under investigation. Gradual deposition of other components of blood like leukocytes, erythrocytes increases the size of the clot leading to thrombosis. Thrombosis can have a detrimental effect on human health by constricting the flow of blood but if it is loosely bound to the endothelial layer, it might lift off with flowing blood and transport to different parts of the body causing stroke. A schematic diagram of the formation of thrombosis is shown below (Figure). In blood contacting medical devices, thrombus formation can lead to the inefficient working of the device and may even lead to failure and eventual rejection of the medical device. Therefore, it is necessary to design and develop blood contacting medical devices that impede the formation of thrombosis. Since thrombosis is a surface driven process, it is of utmost importance to research

on the material surfaces used to make the medical devices and have a strong understanding of the processes that lead to thrombosis and ways that can can be avoided.

1.6 Superhemophobic and superhemophilic titanium surfaces as biomedical implant materials

Contact Angle is the angle between the tangent to the liquid-fluid interface and the tangent to the solid-liquid interface at the triple phase line, measured through the liquid. Contact angle is measured by drawing a tangent on the liquid drop from the point of contact of the solid base. Contact angles can be used to estimate the solid-liquid and solid-vapour interfacial energy and they are particularly easy to measure(contact angle measurement). The interfacial surface tensions are measured using the Young's equation(50) which is stated as follows:

$$\gamma_{lv} \cos \theta = \gamma_{sv} - \gamma_{sl}$$

Where γ_{lv}, γ_{sv},γ_{sl} are the respective liquid-vapor, solid-vapor and solid-liquid interfacial tensions and θ is the apparent contact angle (**Fig 1.6.1**)(50).

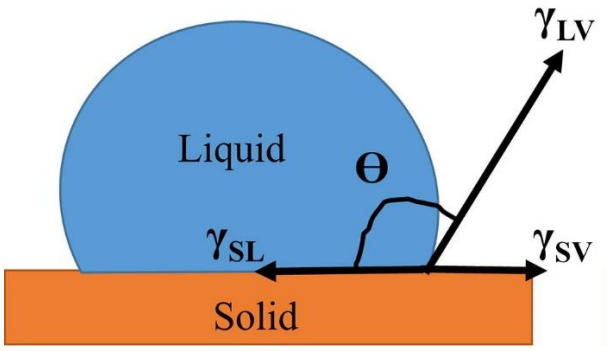

Fig 1.6.1: Representation of Young's model. Reprinted with permission from Elsevier B.V.: Barati Darband G, Aliofkhazraei M, Khorsand S, Sokhanvar S, Kaboli A. Science and Engineering of Superhydrophobic Surfaces: Review of Corrosion Resistance, Chemical and Mechanical Stability. Vol. 13, Arabian Journal of Chemistry. Elsevier B.V.; 2020. p. 1763–802. (51). Copyright (2018) Elsevier B.V. License at http://creativecommons.org/licenses/by-nc-nd/4.0/.

The different surfaces are characterized using their apparent contact angle measurements Surfaces with contact angles less than 10º are called superhydrophilic. If the surfaces show a

contact angle between 10º to 90º, they are hydrophilic and if they show a contact angle between 90º to 150º, they are hydrophobic . Surfaces that show contact angles of more than 150º are superhydrophobic.

Superhemophilic and superhemophobic surfaces are similar to superhydrophobic and superhydrophilic surfaces respectively since the blood contact angles on these surfaces show very similar trends to the contact angle shown with water. Superhemophilic and superhemophobic surfaces are few of the modifications that are prevalent on titanium and titanium surfaces modified with nanostructures. In this study, titania nanotubes are coated with a silane based coating to make it super hydrophobic which has an apparent contact angle of more than 150 for a water droplet. Titania nanotubes are inherently superhemophilic and by modification with a hydrophilic coating makes it hemophilic instead of superhemophilic. Contact angle is measured on each modified surface to determine the nature of each surface.

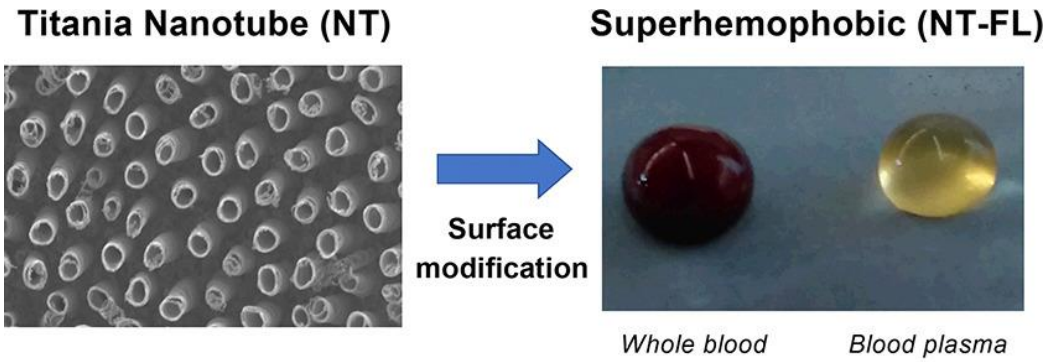

Fig 1.6.2: Representation of Titania Nanotube arrays modified into superhemophobic surfaces (NT-FL). Reprinted from Sabino RM, Kauk K, Movafaghi S, Kota A, Popat KC. Interaction of blood plasma proteins with superhemophobic titania nanotube surfaces. Nanomedicine: Nanotechnology, Biology, and Medicine. 2019 Oct 1;21:102046. Copyright (2019) with permission from Elsevier (49,52–54).

Rough surfaces can be wetted in two conditions, the Wenzel state and the Cassie-Baxter state. Wenzel state refers to a surface interaction where the surface is completely wetted by the surrounding liquid, whereas in Cassie-Baxter state, there is a layer of air trapped between the

surface and the surrounding liquid which results in a lower surface energy and higher contact angles(50). The modified Wenzel equation incorporates the following surface modification factor:

$$\cos \theta_W = r \cos \theta$$

where θ_W is the apparent contact angle in the Wenzel state and r is the ratio of actual surface area to projected surface area (r=1 for a smooth surface and r>1 for a rough surface).

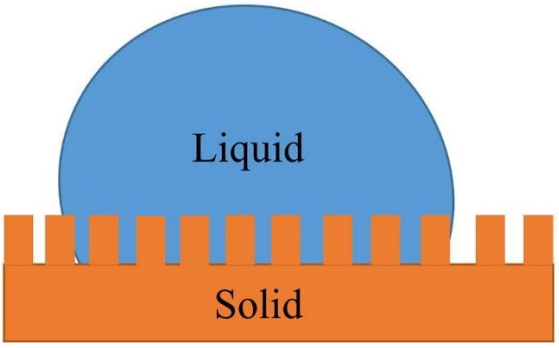

Fig 1.6.3: Representation of Wenzel state. Reprinted with permission from Elsevier B.V.: Barati Darband G, Aliofkhazraei M, Khorsand S, Sokhanvar S, Kaboli A. Science and Engineering of Superhydrophobic Surfaces: Review of Corrosion Resistance, Chemical and Mechanical Stability. Vol. 13, Arabian Journal of Chemistry. Elsevier B.V.; 2020. p. 1763–802. (50). Copyright (2018) Elsevier B.V. License at http://creativecommons.org/licenses/by-nc-nd/4.0/.

With the increase in surface roughness the liquid droplet is in partial contact with the solid surface and a layer of air separates the liquid from completely wetting the solid surface homogeneously. This state is incorporated in the Cassie-Baxter model and is characterized by the following equation:

$$\cos \theta_{CB} = f (1 + \cos \theta) - 1$$

where θ_{CB} is the apparent contact angle in Cassie-Baxter state f is the ratio of the solid-liquid interfacial energy to the liquid-vapor interfacial energy at the solid-liquid interface.

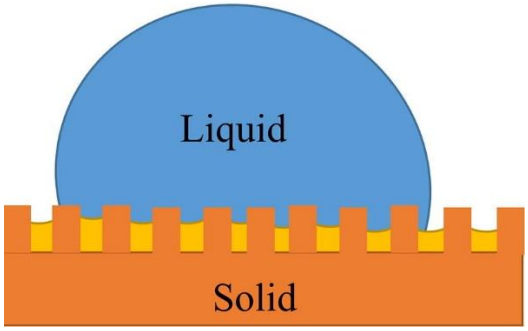

Fig 1.6.4: Representation of Cassie-Baxter state. Reprinted with permission from Elsevier B.V.: Barati Darband G, Aliofkhazraei M, Khorsand S, Sokhanvar S, Kaboli A. Science and Engineering of Superhydrophobic Surfaces: Review of Corrosion Resistance, Chemical and Mechanical Stability. Vol. 13, Arabian Journal of Chemistry. Elsevier B.V.; 2020. p. 1763–802. (55). Copyright (2018) Elsevier B.V. License at http://creativecommons.org/licenses/by-nc-nd/4.0/.

The apparent contact angle for a droplet of liquid on a particular surfaces changes with the advancing or receeding of that droplet either due to evaporation, condensation or movement on an inclined surface. In most cases the the change in apparent contact angle can be as large as 20 degrees(55).

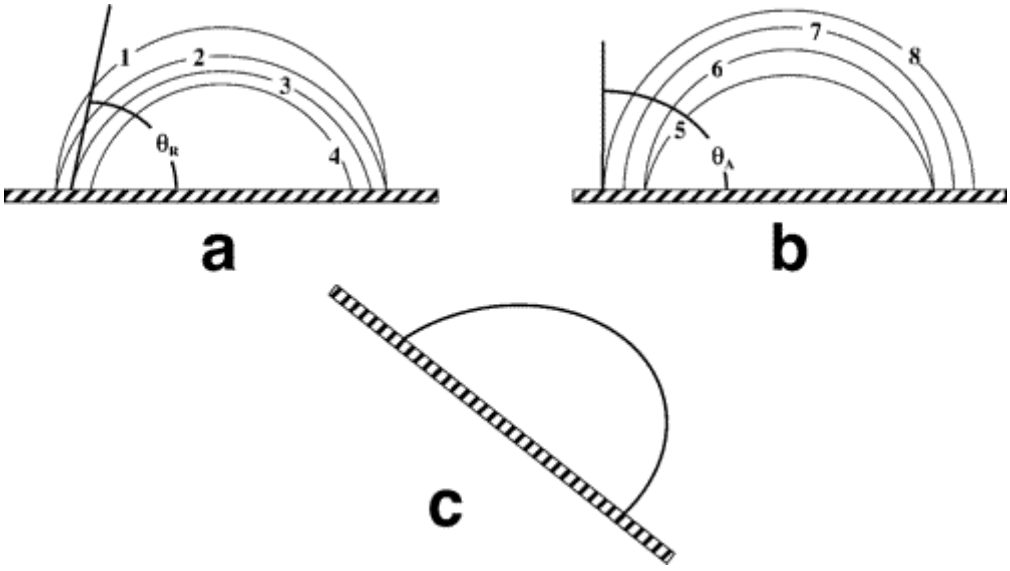

Fig 1.6.5: (a) Receeding contact angle due to evaporation (b) Advancing contact angle due to condensation (c) Change in apparent contact angle due to movement of an inclined surface. Reprinted with permission from Gao L, McCarthy TJ. Contact angle hysteresis explained [Internet]. Vol. 22, Langmuir. American Chemical Society ; 2006 [cited 2020 Oct 9]. p. 6234–7. Available from: https://pubs-acs-org.ezproxy2.library.colostate.edu/doi/full/10.1021/la060254j (55). Copyright (2006) American Chemical Society.

The difference in the advancing and receding contact angle is known as contact angle hysteresis. Hysteresis is an important factor in judging liquid behaviour in specific cases like liquid flow through porous media, surface coatings and adsorption at solid/liquid interfaces(55).

In this study titanium surfaces were modified to form nanotubes on the surface which were further modified to form superhemophobic and hemophilic surfaces. All the surfaces were tested for stability in both static and dynamic conditions using Tyrode solution. Further they were exposed to protein (fibrinogen and albumin) concentrates and PRP in both static and dynamic conditions and compared to each other as well as comparing each surface in static and dynamic conditions to account for the difference in performance in varying conditions. Protein adsorption was quantified using BCA assay and XPS whereas PRP studies (cell adhesion and activation) was quantified using fluorescence microscopy and SEM imaging.

REFERENCES

1. Heron M. National Vital Statistics Reports Volume 68, Number 6, June 24, 2019, Deaths: Leading Causes for 2017 [Internet]. 2019 [cited 2020 May 26]. Available from: https://www.cdc.gov/nchs/products/index.htm.

2. 2020 Heart Disease and Stroke Statistical Update Fact Sheet At-a-Glance Heart Disease, Stroke and other Cardiovascular Diseases.

3. Coronary Heart Disease | NHLBI, NIH [Internet]. [cited 2020 Sep 29]. Available from: https://www.nhlbi.nih.gov/health-topics/coronary-heart-disease

4. Virani SS, Alonso A, Benjamin EJ, Bittencourt MS, Callaway CW, Carson AP, et al. Heart disease and stroke statistics—2020 update: A report from the American Heart Association [Internet]. Vol. 141, Circulation. Lippincott Williams and Wilkins; 2020 [cited 2020 Oct 6]. p. E139–596. Available from: http://ahajournals.org

5. Bainey KR, Norris CM, Graham MM, Ghali WA, Knudtson ML, Welsh RC. Clinical in-stent restenosis with bare metal stents: Is it truly a benign phenomenon? International Journal of Cardiology [Internet]. 2008;128(3):378–82. Available from: http://www.sciencedirect.com/science/article/pii/S0167527307011102

6. Ovid: Abstract 10244: Drug Eluting Balloon - PCI is a New Therapeutic Option for Patients with In - Stent Restenosis in Bare Metal Stents. [Internet]. [cited 2020 Jun 19]. Available from: https://ovidsp-dc2-ovid-com.ezproxy2.library.colostate.edu/sp-4.06.0a/ovidweb.cgi?&S=OCBFFPMDBFEBBBGMJPBKPGHGGHLCAA00&Link+Set=S.sh.22%7c1%7csl_10&Counter5=SS_view_found_article%7c00003017-201111221-00107%7covft%7covftdb%7covftm&Counter5Data=00003017-201111221-00107%7covft%7covftdb%7covftm

7. Hao H, Ishibashi-Ueda H, Tsujimoto M, Ueda Y, Shite J, Gabbiani G, et al. Drug-Eluting Stent. Circulation Journal [Internet]. 2011 Jul [cited 2020 Jun 19];75(7):1548–58. Available from: http://joi.jlc.jst.go.jp/JST.JSTAGE/circj/CJ-11-0393?from=CrossRef

8. Heart Stent Surgery Safety - Heart Health - Everyday Health [Internet]. [cited 2020 May 27]. Available from: https://www.everydayhealth.com/heart-health/the-basics-on-heart-stent-surgery-safety.aspx

9. Saraf AR, Yadav SP. Fundamentals of bare-metal stents. In: Functionalised Cardiovascular Stents. Elsevier; 2018. p. 27–44.

10. Dangas GD, Weitz JI, Giustino G, Makkar R, Mehran R. Prosthetic Heart Valve Thrombosis [Internet]. Vol. 68, Journal of the American College of Cardiology. Elsevier USA; 2016 [cited 2020 Oct 7]. p. 2670–89. Available from: https://pubmed.ncbi.nlm.nih.gov/27978952/

11. Furie B, Furie BC. Mechanisms of Thrombus Formation. New England Journal of Medicine [Internet]. 2008 Aug 28 [cited 2020 Sep 27];359(9):938–49. Available from: http://www.nejm.org/doi/abs/10.1056/NEJMra0801082

12. Kido DK, King PD, Manzione J v., Simon JH. The role of catheters and guidewires in the production of angiographic thromboembolic complications. Investigative Radiology. 1988;23:S359–65.

13. Böswald M, Lugauer S, Bechert T, Greil J, Regenfus A, Guggenbichler JP. Thrombogenicity testing of central venous catheters in vitro. Infection. 1999;27(SUPPL. 1).

14. Hemostasis and Thrombosis: Basic Principles and Clinical Practice - Google Books [Internet]. [cited 2020 Oct 7]. Available from: https://books.google.com/books?hl=en&lr=&id=Tz1V8BS5f-YC&oi=fnd&pg=PR3&dq=Hemostasis+and+thrombosis:+basic+principles+and+clinical+p

ractice&ots=AQe0j53cDI&sig=EVJFoYorLhKz0ygiFNclCAs5itM#v=onepage&q=Hemostasis%20and%20thrombosis%3A%20basic%20principles%20and%20clinical%20practice&f=false

15. Guidewire | definition of guidewire by Medical dictionary [Internet]. [cited 2020 Oct 16]. Available from: https://medical-dictionary.thefreedictionary.com/guidewire

16. Dobbs H. Titanium and its alloys for surgical implants: Phoenix, Arizona, USA, 11–12 May, 1981. Biomaterials [Internet]. 1981;2(4):250. Available from: http://www.sciencedirect.com/science/article/pii/0142961281900715

17. Gordin DM, Ion R, Vasilescu C, Drob SI, Cimpean A, Gloriant T. Potentiality of the “Gum Metal” titanium-based alloy for biomedical applications. Materials Science and Engineering: C [Internet]. 2014;44:362–70. Available from: http://www.sciencedirect.com/science/article/pii/S0928493114004883

18. Semlitsch M. Titanium alloys for hip joint replacements. Clinical Materials [Internet]. 1987;2(1):1–13. Available from: http://www.sciencedirect.com/science/article/pii/0267660587900151

19. Ghosh S, Abanteriba S, Wong S, Houshyar S. Selective laser melted titanium alloys for hip implant applications: Surface modification with new method of polymer grafting. Journal of the Mechanical Behavior of Biomedical Materials [Internet]. 2018;87:312–24. Available from: http://www.sciencedirect.com/science/article/pii/S1751616118308403

20. Li P, Li L, Wang W, Jin W, Liu X, Yeung KWK, et al. Enhanced corrosion resistance and hemocompatibility of biomedical NiTi alloy by atmospheric-pressure plasma polymerized fluorine-rich coating. Applied Surface Science [Internet]. 2014;297:109–15. Available from: http://www.sciencedirect.com/science/article/pii/S0169433214001329

21. 7. Metals and alloys for biomedical applications | Elsevier Enhanced Reader [Internet]. [cited 2020 Oct 3]. Available from: https://reader.elsevier.com/reader/sd/pii/B9780081022054000076?token=F5BF5CB1B5CAEF2A4C5BF131D852942EE01505AE45F6AD1885095AB1C741EEE14C704744A7357D40570A36AFBECCE498

22. Bartlet K, Movafaghi S, Kota A, Popat KC. Superhemophobic titania nanotube array surfaces for blood contacting medical devices. RSC Advances [Internet]. 2017 Jul 11 [cited 2020 Oct 5];7(56):35466–76. Available from: https://pubs-rsc-org.ezproxy2.library.colostate.edu/en/content/articlehtml/2017/ra/c7ra03373g

23. Lin WC, Liu TY, Yang MC. Hemocompatibility of polyacrylonitrile dialysis membrane immobilized with chitosan and heparin conjugate. Biomaterials [Internet]. 2004 [cited 2020 Oct 7];25(10):1947–57. Available from: https://pubmed.ncbi.nlm.nih.gov/14738859/

24. Chou CC, Hsin SW, Lin HC, Yeh CH, Wu R, Cherng WJ. Oxidized dopamine as the interlayer between heparin/collagen polyelectrolyte multilayers and titanium substrate: An investigation of the coating's adhesion and hemocompatibility. Surface and Coatings Technology. 2016 Oct 15;303:277–82.

25. Chou CC, Zeng HJ, Yeh CH. Blood compatibility and adhesion of collagen/heparin multilayers coated on two titanium surfaces by a layer-by-layer technique. In: Thin Solid Films. Elsevier; 2013. p. 117–22.

26. Weber N, Wendel HP, Ziemer G. Hemocompatibility of heparin-coated surfaces and the role of selective plasma protein adsorption. Biomaterials [Internet]. 2002 [cited 2020 Oct 7];23(2):429–39. Available from: https://pubmed.ncbi.nlm.nih.gov/11761163/

27. Zheng Z, Wang W, Huang X, Lv Q, Fan W, Yu W, et al. Fabrication, Characterization, and Hemocompatibility Investigation of Polysulfone Grafted With Polyethylene Glycol and

Heparin Used in Membrane Oxygenators. Artificial Organs [Internet]. 2016 Nov 1 [cited 2020 Oct 7];40(11):E219–29. Available from: https://pubmed.ncbi.nlm.nih.gov/28374499/

28. Smith BS, Capellato P, Kelley S, Gonzalez-Juarrero M, Popat KC. Reduced in vitro immune response on titania nanotube arrays compared to titanium surface. Biomaterials Science. 2013 Mar 4;1(3):322–32.

29. Smith BS, Yoriya S, Grissom L, Grimes CA, Popat KC. Hemocompatibility of titania nanotube arrays. Journal of Biomedical Materials Research Part A [Internet]. 2011 Mar 1 [cited 2020 Jun 12];96A(3):608–608. Available from: http://doi.wiley.com/10.1002/jbm.a.33004

30. Bartlet K, Movafaghi S, Kota A, Popat KC. Superhemophobic titania nanotube array surfaces for blood contacting medical devices. RSC Advances. 2017 Jul 17;7(56):35466–76.

31. Smith BS, Yoriya S, Grissom L, Grimes CA, Popat KC. Hemocompatibility of titania nanotube arrays. Journal of Biomedical Materials Research - Part A. 2010 Nov;95 A(2):350–60.

32. Damodaran VB, Bhatnagar D, Leszczak V, Popat KC. Titania nanostructures: A biomedical perspective [Internet]. Vol. 5, RSC Advances. Royal Society of Chemistry; 2015 [cited 2020 Oct 3]. p. 37149–71. Available from: www.rsc.org/advances

33. Galstyan V, Comini E, Faglia G, Sberveglieri G. TiO2 nanotubes: Recent advances in synthesis and gas sensing properties [Internet]. Vol. 13, Sensors (Switzerland). MDPI AG; 2013 [cited 2020 Oct 7]. p. 14813–38. Available from: https://pubmed.ncbi.nlm.nih.gov/24184919/

34. Thorwarth G, Saldamli B, Schwarz F, Jürgens P, Leiggener C, Sader R, et al. Biocompatibility of Doped Diamond-Like Carbon Coatings for Medical Implants. Plasma Processes and Polymers [Internet]. 2007 Apr 1 [cited 2020 Oct 25];4(S1):S364–8. Available from: http://doi.wiley.com/10.1002/ppap.200731001

35. Peng L, Eltgroth ML, LaTempa TJ, Grimes CA, Desai TA. The effect of TiO2 nanotubes on endothelial function and smooth muscle proliferation. Biomaterials [Internet]. 2009 Mar [cited 2020 Oct 7];30(7):1268–72. Available from: https://pubmed.ncbi.nlm.nih.gov/19081625/

36. Park J, Bauer S, Schmuki P, von der Mark K. Narrow window in nanoscale dependent activation of endothelial cell growth and differentiation on TiO2 nanotube surfaces. Nano Letters [Internet]. 2009 Sep 9 [cited 2020 Oct 7];9(9):3157–64. Available from: https://pubmed.ncbi.nlm.nih.gov/19653637/

37. Brammer KS, Oh S, Gallagher JO, Jin S. Enhanced cellular mobility guided by TiO2 nanotube surfaces. Nano Letters [Internet]. 2008 Mar [cited 2020 Oct 7];8(3):786–93. Available from: https://pubmed.ncbi.nlm.nih.gov/18251515/

38. Jaffer IH, Fredenburgh JC, Hirsh J, Weitz JI. Medical device-induced thrombosis: What causes it and how can we prevent it? [Internet]. Vol. 13, Journal of Thrombosis and Haemostasis. Blackwell Publishing Ltd; 2015 [cited 2020 Sep 27]. p. S72–81. Available from: https://onlinelibrary.wiley.com/doi/full/10.1111/jth.12961

39. (No Title) [Internet]. [cited 2020 Oct 7]. Available from: http://www.terumo-cvgroup.com/doc/Schiel_CanadianPerfusionCanadienne_11_No2.pdf

40. Kasemo B. Biological surface science. Surface Science. 2002 Mar 10;500(1–3):656–77.

41. Carré A, Lacarrière V. How substrate properties control cell adhesion. A physical-chemical approach. Journal of Adhesion Science and Technology. 2010 Apr 1;24(5):815–30.

42. Parhi P, Golas A, Vogler EA. Role of proteins and water in the initial attachment of mammalian cells to biomedical surfaces: A review. Journal of Adhesion Science and Technology. 2010 Apr 1;24(5):853–88.

43. Scopus - Document details [Internet]. [cited 2020 Oct 7]. Available from: https://www.scopus.com/record/display.uri?eid=2-s2.0-84935420977&origin=inward&txGid=fd115d1e1f572532a2a7c2904ef04436

44. Tsapikouni TS, Missirlis YF. Protein-material interactions: From micro-to-nano scale. Vol. 152, Materials Science and Engineering B: Solid-State Materials for Advanced Technology. 2008. p. 2–7.

45. Ponche A, Ploux L, Anselme K. Protein/material interfaces: Investigation on model surfaces. Journal of Adhesion Science and Technology. 2010 Sep 1;24(13–14):2141–64.

46. Silva-Bermudez P, Rodil SE. An overview of protein adsorption on metal oxide coatings for biomedical implants. Vol. 233, Surface and Coatings Technology. Elsevier; 2013. p. 147–58.

47. Amara U, Rittirsch D, Flierl M, Bruckner U, Klos A, Gebhard F, et al. Interaction between the coagulation and complement system [Internet]. Vol. 632, Advances in Experimental Medicine and Biology. Springer New York; 2008 [cited 2020 Oct 7]. p. 71–9. Available from: https://link-springer-com.ezproxy2.library.colostate.edu/chapter/10.1007/978-0-387-78952-1_6

48. Vu TKH, Hung DT, Wheaton VI, Coughlin SR. Molecular cloning of a functional thrombin receptor reveals a novel proteolytic mechanism of receptor activation. Cell. 1991 Mar 22;64(6):1057–68.

49. Yan YY, Gao N, Barthlott W. Mimicking natural superhydrophobic surfaces and grasping the wetting process: A review on recent progress in preparing superhydrophobic surfaces. Vol. 169, Advances in Colloid and Interface Science. Elsevier B.V.; 2011. p. 80–105.

50. Barati Darband G, Aliofkhazraei M, Khorsand S, Sokhanvar S, Kaboli A. Science and Engineering of Superhydrophobic Surfaces: Review of Corrosion Resistance, Chemical and Mechanical Stability. Vol. 13, Arabian Journal of Chemistry. Elsevier B.V.; 2020. p. 1763–802.

51. Sabino RM, Kauk K, Movafaghi S, Kota A, Popat KC. Interaction of blood plasma proteins with superhemophobic titania nanotube surfaces. Nanomedicine: Nanotechnology, Biology, and Medicine. 2019 Oct 1;21:102046.

52. Wenzel RN. Resistance of solid surfaces to wetting by water. Industrial and Engineering Chemistry [Internet]. 1936 Aug 1 [cited 2020 Oct 7];28(8):988–94. Available from: https://pubs.acs.org/doi/abs/10.1021/ie50320a024

53. Cassie ABD, Baxter S. Wettability of porous surfaces. Transactions of the Faraday Society [Internet]. 1944 Jan 1 [cited 2020 Oct 7];40(0):546–51. Available from: https://pubs.rsc.org/en/content/articlehtml/1944/tf/tf9444000546

54. Barati Darband G, Aliofkhazraei M, Khorsand S, Sokhanvar S, Kaboli A. Science and Engineering of Superhydrophobic Surfaces: Review of Corrosion Resistance, Chemical and Mechanical Stability. Vol. 13, Arabian Journal of Chemistry. Elsevier B.V.; 2020. p. 1763–802.

55. Gao L, McCarthy TJ. Contact angle hysteresis explained [Internet]. Vol. 22, Langmuir. American Chemical Society ; 2006 [cited 2020 Oct 9]. p. 6234–7. Available from: https://pubs-acs-org.ezproxy2.library.colostate.edu/doi/full/10.1021/la060254j

CHAPTER 2

FABRICATION AND CHARACTERIZATION OF TITANIA NANOTUBE SURFACES

2.1 Introduction

Ti is widely used as an implant material for blood contacting medical devices and is known to be relatively hemocompatible(1–4), however it still cannot prevent thrombus formation with prolonged exposure to blood. Many surface modification strategies have been investigated to improve hemocompatibility of Ti surface. In this study, Ti was modified using electrochemical anodization to create nanotubes on the surface since previous studies have shown that these NT surfaces are very effective in improving hemocompatibility under static conditions(5–7). The electrolytic solution for the anodization contains hydrofluoric acid which erodes the surface to form nanotubes. Selective etching on the surface of Ti resulted in pits followed by chemical dissolution which resulted in the nanopores. These nanopores were allowed to grow for 22 hours to attain tubular geometries thus resulting in nanotubes on the surface. Both the Ti and NT surfaces were further silanized with Heptadecafluoro-1,1,2,2-tetrahydrodecyl(Trichlorosilane) (Silane) to make surface superhydrophobic, and PEGylated with 2-[methoxy(polyethyleneoxy)6-9propyl]trimethoxysilane (PEG) to make the surface superhydrophilic (**Figure 2.1.1**). The stability of these surfaces were investigated in both static and dynamic conditions by exposing them to Hepes-tyrode solution.

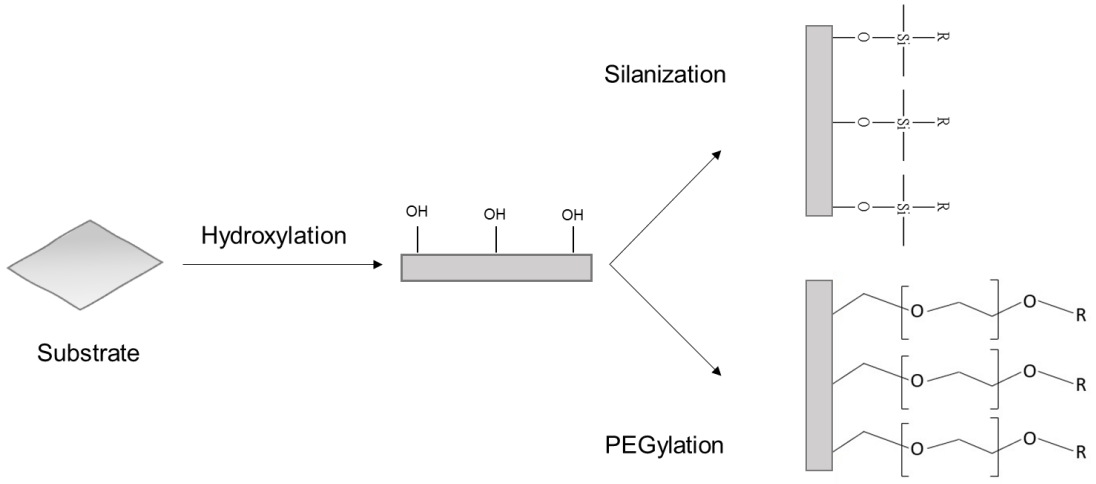

Figure 2.1.1: Schematic of modification procedure for different surfaces.

2.2 Materials and Methods

2.2.1. Fabrication of titania nanotube arrays

Titanium sheets of 0.020" thickness were cut into square pieces of 2cm X 2cm for the fabrication of titania nanotube arrays. The cut pieces were cleaned with acetone, isopropyl alcohol and DI water before drying it inside the fume hood for 10 minutes. The pre-cut platinum foil was cleaned similarly before anodization. After the cleaning procedures, the titanium and platinum pieces were placed inside an electrolytic solution made of 95% Diethylene glycol (DEG, basic, 99% reagent, Sigma), 2% HF solution (48% HF solution), 3% deionized H_2O(8). It was made sure that the two materials were at least 15-20 mm apart. The circuit was completed so that the positive terminal was connected to titanium and the negative to platinum, and was run at 55V for 22 hours.

After 22 hours the pieces were washed with DI water followed by isopropyl alcohol and clean DI water again. They were marked to distinguish the side where nanotube arrays were formed. After that, the surfaces with nanotubes were placed inside an oven, facing up. The surfaces were annealed at a rate of 15^{o}C/min and holding the temperature at 530^{o}C for 3 hours.

The titania nanotube arrays (denoted as NT) were cleaned with plasma inside an oxygen plasma chamber for 15 minutes before further surface modification as mentioned below:

- Titania nanotube arrays were kept on a hot plate with Heptadecafluoro-1,1,2,2-tetrahydrodecyl (Trichlorosilane) for 55 minutes at a temperature of 140°C to make them superhydrophobic (denoted as NT-S).
- Titania nanotube arrays submerged in a solution made of 200 µL 2-[methoxy(polyethyleneoxy)6-9propyl]trimethoxysilane and 10 mL ethanol, and kept for 22 hours to make then superhydropphilic (NT-PEG). After 22 hours, the surfaces were washed with ethanol followed by DI water.

2.2.2 Surface characterization

The surface topography was characterised using a JEOL 6500 field emission SEM (Scanning Electron Microscope) operated at an accelerating voltage of 15KV. The surfaces were imaged at a magnification of 500X, 2000X and 10000X.

The surface wettability was characterized by measuring apparent contact angle (θ^*) at room temperature on a Ramé-hart 260F4 goniometer. Images were taken after the 5 µl water droplet was placed on the surface was stable (3 seconds after the droplet was placed). The images were then analyzed using the manufacturer provided software for measuring contact angles.

Advancing and receding contact angle was measured by a Ramé-hart 260F4 goniometer to calculate surface contact angle hysteresis. A polar liquid(water) and a non-polar liquid (Hexadecane) was used. The advancing contact angle was used to calculate the solid-liquid surface energy with the following equations:

$$\gamma_{lv} \cos\theta = \gamma_{sv} - \gamma_{sl} \text{ (Young's equation)}$$

$$\gamma_{sl} = \gamma_{sv} + \gamma_{lv} - 2\left(\sqrt{\gamma_{sv}^{D}\gamma_{lv}^{D}} + \sqrt{\gamma_{sv}^{P}\gamma_{lv}^{P}}\right) \text{(Owens-Wendt equation)}$$

The surface chemistry was characterized using a PE-5800 X-ray Photoelectron spectrometer (XPS). Survey spectra were collected for binding energy of 10 to 1100 eV and with

the pass energy is 187 eV. Carbon high resolution surveys (C1s) were collected with a pass energy of 10 eV. The elemental surface composition on the surfaces were calculated using peak fit analysis of the Multipak and Origin software.

The stability of the different surfaces were evaluated by exposing the surfaces to dynamic flow conditions in a flow chamber (Section 2.3 for more details about flow chamber) and comparing the results with static immersion of surfaces in Tyrode solution. For static study, the surfaces were incubated in Tyrode for 2 hours and then cleaned three times with PBS. For dynamic study, the surfaces were placed in the dynamic chamber and Tyrode solution was flowed on them at a constant flow rate of 20 ml/hr for 2 hours (maximum possible for a 50 ml syringe). The surfaces then were cleaned three times with PBS. Following the stability studies, the surfaces were characterized using SEM, contact angle measurements and XPS as described above.

2.2.3. Flow chamber design and development

The Dynamic Chamber was designed to have a steady laminar flow over the substrates placed inside them. It was made up of three parts, namely the two acrylic plates and the rubber gasket in between then to prevent leakage from the chamber. The bottom plate was designed to carry the substrate, the vacuum channels and the exit channel for the fluid to flow to the sink. The top plate consists of an inlet for the fluid (e.g. Tyrode solution, protein solution, platelet rich plasma (PRP)) to flow into the chamber. The fluid is flowed for 30 mins on each surface at a fixed shear through the chamber at a fixed rate of 20 ml/hr inside the biosafety cabinet at room temperature using a high precision syringe pump (NE-1000). 60 ml syringe were used to load the fluid on the syringe pump. The Reynold's number analysed for the flow chamber was found to be 1.034, thus proving the flow inside the chamber is laminar.

$$\mathrm{Re} = \frac{\rho u D_\mathrm{H}}{\mu} = \frac{u D_\mathrm{H}}{\nu} = \frac{Q D_\mathrm{H}}{\nu A} = \frac{W D_\mathrm{H}}{\mu A}$$

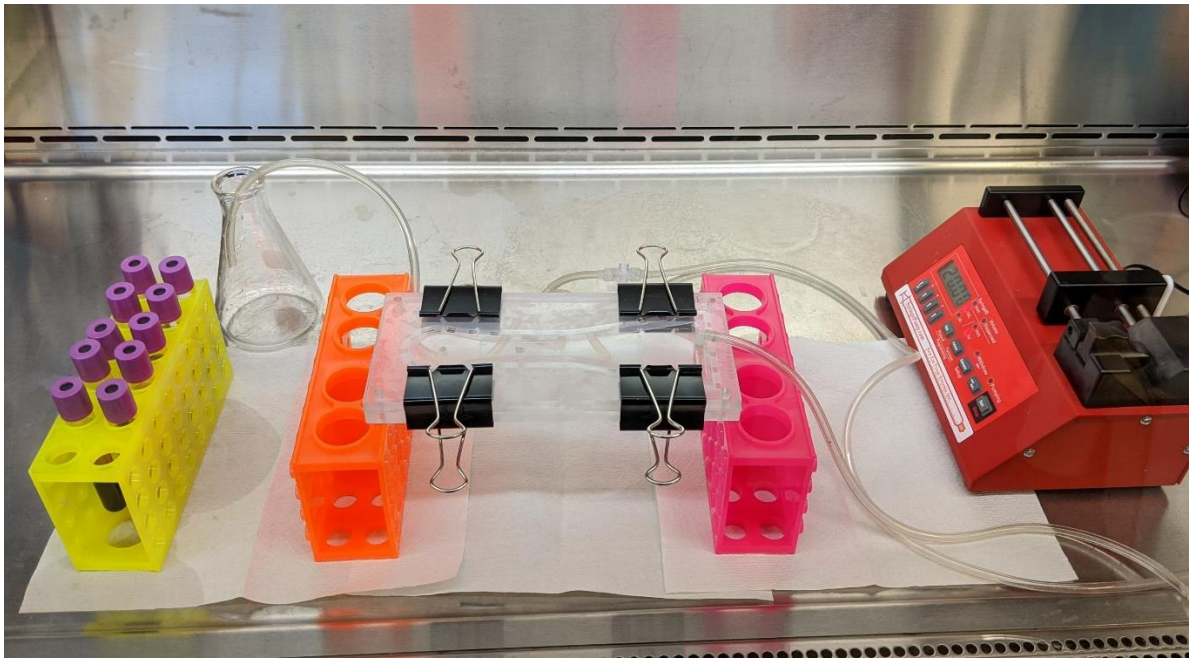

Fig 2.2.1: Dynamic flow chamber for Protein and PRP studies.

2.2.4 Statistical analysis

Every analysis was carried out in repetitions of at least three times to find their mean and variability. Surface characterization was done on at least three different places on a surface. SEM images were taken at least on three different locations on each surface. Exposure to Tyrode for stability testing in both static and dynamic conditions were repeated at least three times. Contact angle was measured at least at three different locations on a surface after fabrication and on three different samples after static and dynamic stability testing. The results were analysed using a software JMP Pro to find ANOVA and student's t test. Statistical significance was calculated using JMP Pro using a 0.95 probability of occurrence.

2.3. Results and Discussion

2.3.1. Surface morphology

The morphology of the different surfaces was characterized using SEM to evaluate the uniformity of the surfaces. The SEM images of Ti show the surface morphology as expected. Ti hade some imperfections due to the surface roughness and the presence of grain boundaries but was uniform throughout the entire surface (**Figure 2.3.1**). After surface modification, there was not any significant difference in the morphology of Ti surfaces. Further, the NT surfaces showed perpendicular nanotubular structures with uniform length and diameter throughout the surface with no significant changes after surface modification. The length and diameter of the nanotubes were calculated using ImageJ software and they were approximately the same before and after modification. The length of the nanotubes was 1 ± 0.2 µm and their diameter was 160 ± 5 nm. Thus, the results indicate that the surface modifications have not changed the morphology of the surfaces.

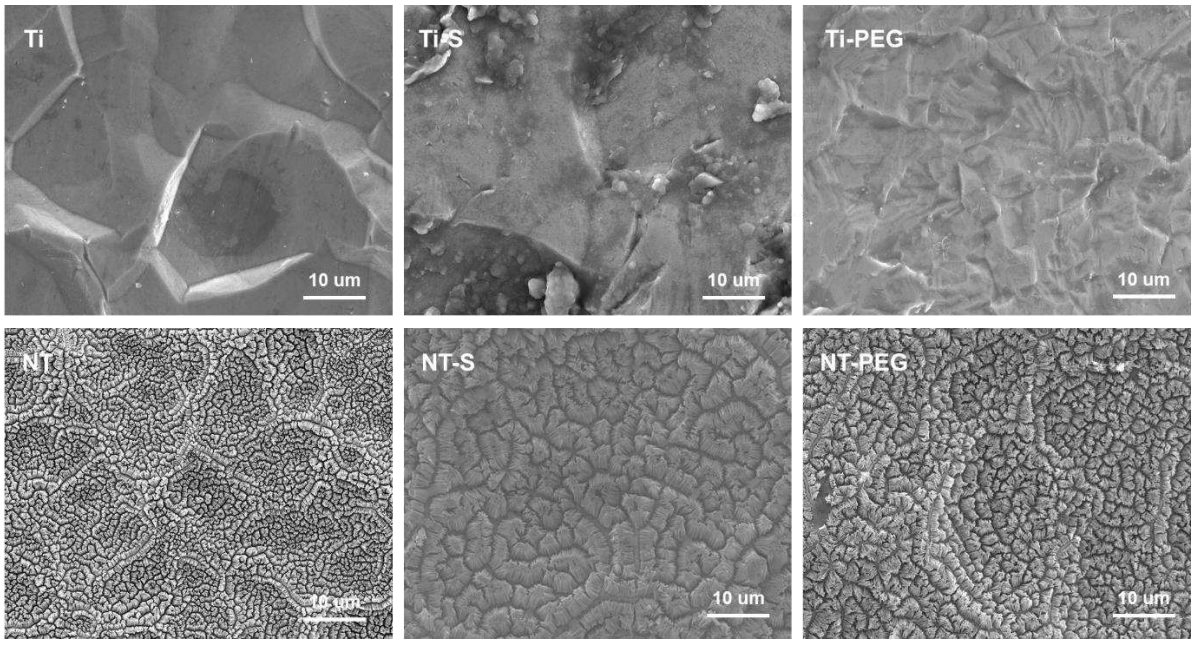

Figure 2.3.1: Representative SEM images of different surfaces.

2.3.2. Surface wettability

The wettability of the surfaces was characterized by measuring the apparent contact angles using a goniometer. Water was used to measure the apparent contact angle for the

surfaces since it is a common polar fluid and is a major component of blood. Surfaces with contact angles less then 10º are called superhydrophilic. If the surfaces show a contact angle between 10º to 90º, they are hydrophilic and if they show a contact angle between 90º to 150º, they are hydrophobic. Surfaces that show contact angles of more than 150º are superhydrophobic. Hydrophilic surfaces are formed due to higher surface energies resulting in higher interaction with the surrounding atmosphere. The contact angles were measured on the surfaces immediately after fabrication. The contact angles were also measured on surfaces after static and dynamic exposure of Hepes-Tyrode solution. The results from as fabricated surfaces indicated a contact angle of 62º ± 8º for Ti, indicating hydrophilic surface; 110º ± 5º for Ti-S indicating hydrophobic surface; and 49º ± 2º for Ti-PEG indicating hydrophilic surface (**Figure 2.3.2A**). For nanostructured surfaces like NT, contact angle can be defined two different kinds of solid-liquid surface interactions, namely the Wenzel state and the Cassie-Baxter state. Wenzel state refers to a surface interaction where the surface is completely wetted by the surrounding liquid, whereas in Cassie-Baxter state, there is a layer of air trapped between the surface and the surrounding liquid which results in a lower surface energy and higher contact angles. The contact angle of NT was close to 0º indicating a superhydrophilic surface under Wenzel state. On the contrary, the contact angle of NT-S was 153º ± 1º indicating a superhydrophobic surface. The surface modification of NT surfaces with high surface energy chemical species resulted in Cassie-Baxter state. The NT surfaces after modifying with silane creates secondary chain structures on the nanotextures already present on the surface, resulting in a layer of air in between the liquid and the solid as air is trapped in between the structures, thus resulting in the solid-liquid interaction to be in Cassie-Baxter state. The contact angle of NT-PEG was 65º ± 1º indicating hydrophilic surface. The contact angles for all the surfaces after exposure to Hepes-Tyrode solution (dynamic and static) were statistically similar to that of as-fabricated surfaces (**Figure 2.3.2B**). Further, the contact angles followed a trend of NT-S>Ti-S>Ti>NT-PEG>Ti-PEG>NT and the values were all statistically different from each other.

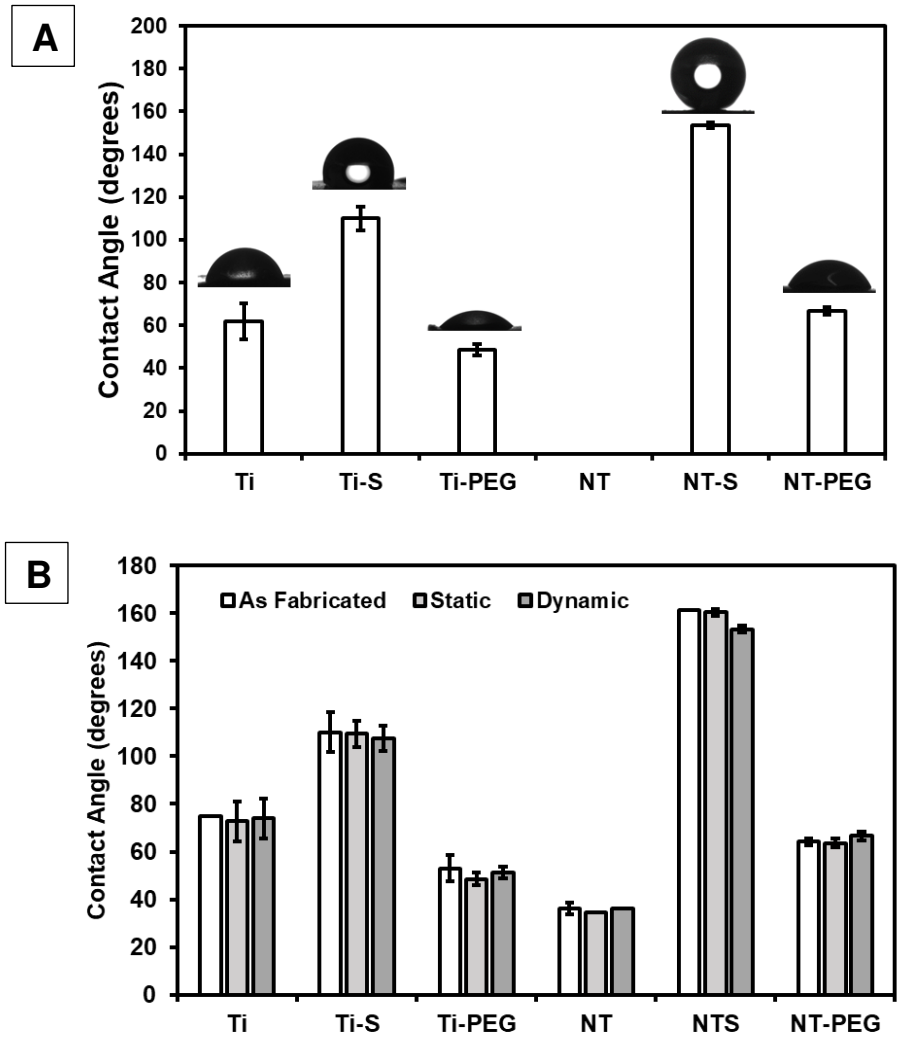

Figure 2.3.2: (A) Static contact angles of human blood plasma for different substrates. Significant differences in contact angles for all surfaces ($p < 0.05$). (B) Static contact angles for all surfaces as fabricated, after static stability test and after dynamic stability test.

The surface energy of different surfaces was calculated using Owen-Wendt equation by measuring the advancing contact angle immediately after fabrication of surfaces. Advancing contact angle was measured using a polar liquid (water) and a non-polar liquid (hexadecane). Surface energy is inversely proportional to the contact angle of the surface. Thus, a higher energy surfaces will be hydrophilic and a lower energy surfaces will be hydrophobic. In this study, NT

was found to be possessing the highest surface energy whereas NT-S had the lowest surface energy which exactly followed the trend of contact angles observed while testing surface wettability where NT had the least contact angle whereas NT-S had the highest contact angle of all surfaces (**Table 2.3.1**).

Table 2.3.1: Surfaces energies of the different surfaces in mN/m.

Ti	28.54
Ti-S	9.36
Ti-PEG	28.79
NT	32.46
NT-S	1.03
NT-PEG	N/A

2.3.3. Surface chemistry

The chemistry of different surfaces was characterized by XPS. XPS was chosen as the surface modification resulted in very thin films of the surface. Survey scans were taken for all surfaces immediately after fabrication and again after flowing Hepes-Tyrode solution on the surfaces (dynamic stability) (**Figure 2.3.3A & 2.3.3B**). XPS characterization was not done after static stability since the contact angle values were very similar were very similar to that of as fabricated surfaces. The results indicated presence of titanium, Ti2p (458.5 eV) and oxygen, O1s (529-530 eV for metal oxides) on all as fabricated surfaces due to the oxide layer formed on it. The surfaces also showed presence of carbon, C1s (284 eV) which most likely was from impurities on the surface due to exposure in XPS chamber. The survey scans for Ti-S indicated presence of distinctive fluorine peaks, F1s due to their surface modification using a fluorine-based silane. Further, both Ti-S and Ti-PEG had traces of silicon, Si2p and chlorine, Cl2p peaks resulting from its respective modifications. NT showed a very similar surface chemistry to that of Ti with the only difference of much reduced presence of C1s peak on the surface due to anodization of Ti surface.

NT-S and NT-PEG showed very similar surface characteristics to Ti-S and Ti-PEG respectively. All of the surfaces showed O1s peaks, however, they were highest for the Ti-PEG and the NT-PEG. After dynamic stability, XPS was done again and the results indicate almost similar to that of as fabricated indicating that the surfaces are stable. The survey scans obtained from the XPS were processed using Multipak and Origin softwares. Further, the thickness of the surface modifications was calculated using the standard overlayer method given by the equation as follows:

$$I_{Ti} = I^{0}_{Ti}\, exp\ (-t/L_{Ti})$$

Where I^{0}_{Ti} is the intensity of the Ti2p peak before modification, I_{Ti} is the intensity peak of Ti2p after modification, t is the thickness of the modification and L_{Ti} is the electron attenuation for the Ti2p peak. The attenuation length of the Ti2p peak was found to be 2.1 nm. From the XPS results, the peak values of Ti2p (approx. peak at 455 eV) were obtained and the thicknesses for the modifications were calculated as 0.405 nm and 0.098 nm for the hydrophobic and hydrophilic coatings respectively. This can be further verified from the SEM images where the coatings are barely visible since they are very thin.

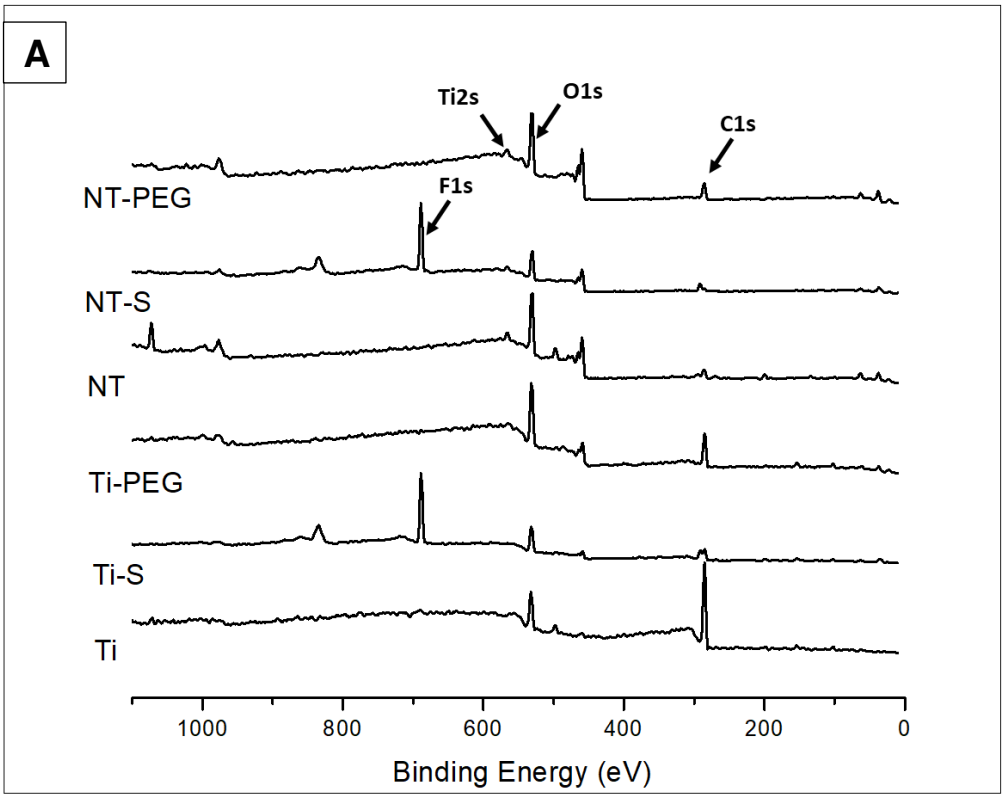
A
Ti2s
O1s
C1s
F1s
NT-PEG
NT-S
NT
Ti-PEG
Ti-S
Ti
1000
800
600
400
200
0
Binding Energy (eV)

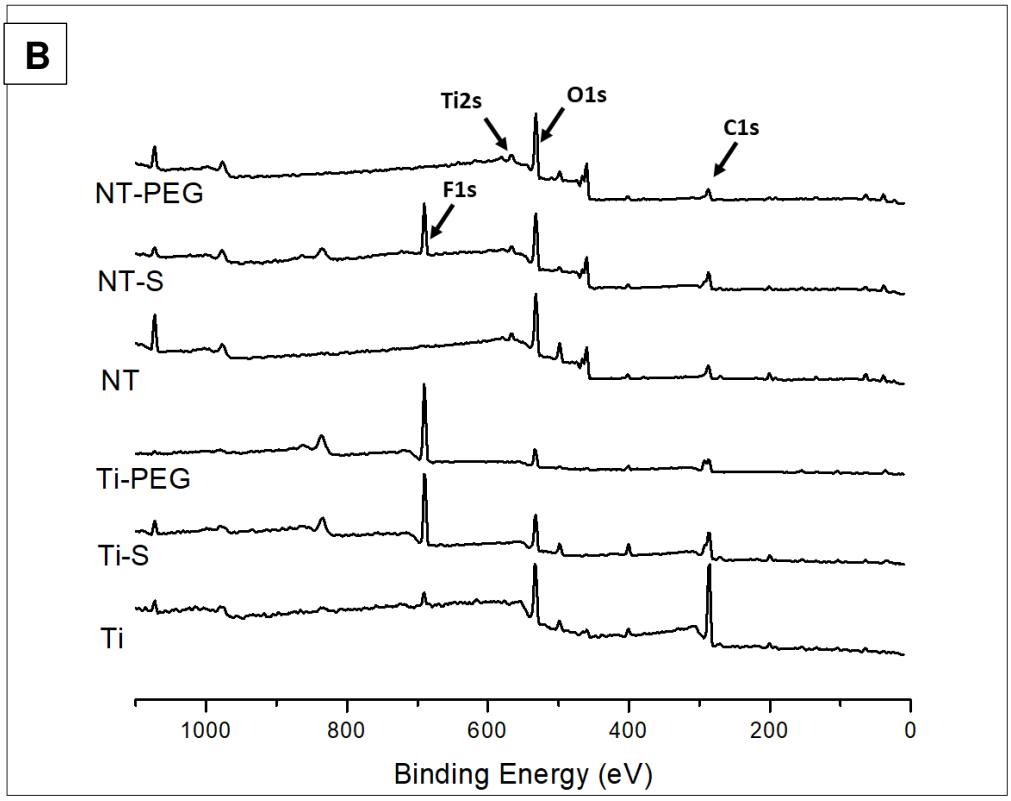
B
Ti2s
O1s
C1s
F1s
NT-PEG
NT-S
NT
Ti-PEG
Ti-S
Ti
1000
800
600
400
200
0
Binding Energy (eV)

Figure 2.3.3: Representative XPS survey scans for (A) As fabricated surfaces. (B) after dynamic stability for all surfaces.

Table 2.3.2: Adsorption percentages of different materials on the surfaces before (B) and after (A) stability testing.

Comparison B/A

	O1s		F1s		Si2p		Cl2p		Ti2p		C1s	
	B	A	B	A	B	A	B	A	B	A	B	A
Ti	20.8	1	0	0	0	0	0	0	2.8	73.9	76.4	25.11
Ti-S	19.82	13.89	37.84	43.13	4.8	2.7	0.91	1.11	1.96	1.42	34.68	36.25
Ti-PEG	38.99	33.02	0	5.28	6.02	3.3	0.12	0.06	5.91	0.7	48.96	56.48
NT	63.15	57.72	0	0	0	0	0	0	15.11	10.01	21.73	32.28
NT-S	25.46	35.94	45.78	23.15	0.5	1.16	0.11	1.43	7.81	6.79	20.35	31.53
NT-PEG	49.32	59.53	0.37	0	2.94	0.13	0	0.24	15.26	11.9	32.12	28.2

2.4 Conclusion

The contact angles of the different surfaces show they all have significantly different surface characteristics to each other. Although they are different from each other, they showed very similar trends and very little variability when compared before and after stability testing which indicates that all the surfaces are stable and consistent in the different conditions they are exposed to.

REFERENCES

1. Dobbs H. Titanium and its alloys for surgical implants: Phoenix, Arizona, USA, 11–12 May, 1981. Biomaterials [Internet]. 1981;2(4):250. Available from: http://www.sciencedirect.com/science/article/pii/0142961281900715
2. Gordin DM, Ion R, Vasilescu C, Drob SI, Cimpean A, Gloriant T. Potentiality of the “Gum Metal” titanium-based alloy for biomedical applications. Materials Science and Engineering: C [Internet]. 2014;44:362–70. Available from: http://www.sciencedirect.com/science/article/pii/S0928493114004883
3. Semlitsch M. Titanium alloys for hip joint replacements. Clinical Materials [Internet]. 1987;2(1):1–13. Available from: http://www.sciencedirect.com/science/article/pii/0267660587900151
4. Li P, Li L, Wang W, Jin W, Liu X, Yeung KWK, et al. Enhanced corrosion resistance and hemocompatibility of biomedical NiTi alloy by atmospheric-pressure plasma polymerized fluorine-rich coating. Applied Surface Science [Internet]. 2014;297:109–15. Available from: http://www.sciencedirect.com/science/article/pii/S0169433214001329
5. Smith BS, Capellato P, Kelley S, Gonzalez-Juarrero M, Popat KC. Reduced in vitro immune response on titania nanotube arrays compared to titanium surface. Biomaterials Science. 2013 Mar 4;1(3):322–32.
6. Bartlet K, Movafaghi S, Kota A, Popat KC. Superhemophobic titania nanotube array surfaces for blood contacting medical devices. RSC Advances [Internet]. 2017 Jul 11 [cited 2020 Oct 5];7(56):35466–76. Available from: https://pubs-rsc-org.ezproxy2.library.colostate.edu/en/content/articlehtml/2017/ra/c7ra03373g
7. Smith BS, Yoriya S, Grissom L, Grimes CA, Popat KC. Hemocompatibility of titania nanotube arrays. Journal of Biomedical Materials Research - Part A. 2010 Nov;95 A(2):350–60.

8. Sabino RM, Kauk K, Movafaghi S, Kota A, Popat KC. Interaction of blood plasma proteins with superhemophobic titania nanotube surfaces. Nanomedicine: Nanotechnology, Biology, and Medicine. 2019 Oct 1;21:102046.

CHAPTER 3

PROTEIN ADSORPTION ON TITANIA NANOTUBE SURFACES IN STATIC AND DYNAMIC CONDITIONS

3.1. Introduction

Protein adsorption is initiated when blood and its components contact a synthetic surface(1–3). Protein adsorption initiates the contact activation which is seen when blood comes in contact with non-endothelial surfaces(4). Protein adsorption is a major clotting factor for blood contacting surfaces as the adsorption of proteins like fibrinogen induces the clotting cascade. Albumin, on the other hand is the most abundant protein present in blood. In this study the different surfaces were exposed to fibrinogen and albumin and their interaction with proteins was investigated under dynamic flow conditions and compared to the results from static conditions.

3.2 Materials and Methods

3.2.1 Static vs. dynamic studies on different surfaces

Static studies were done by incubating the surfaces in a 48-well plate with 300 µl fluid (Tyrode solution, protein solution, platelet rich plasma (PRP)) for 2 hours on a shaker at 100 rpm inside an incubator with fixed conditions of 37°C and 5% CO_2. The surfaces were then cleaned with PBS three times and characterized as discussed below.

Dynamic studies were done by placing the substrates inside the flow chamber and flowing fluid (Tyrode solution/protein solution/platelet rich plasma) through the flow chamber at a constant rate of 20 ml/hr for 30 minutes for each sample inside the bio-hood. The surfaces were then cleaned with PBS three times and characterized as discussed below.

3.2.2 Protein adsorption

Albumin and Fibrinogen adsorption on the different surfaces was characterised with a micro-BCA assay. The surfaces were incubated with 300 µl of 100 µg/ml protein solution in PBS for static studies and were kept in the flow chamber with the same concentration of protein solution for dynamic studies. After exposing the surfaces to protein, the surfaces are cleaned with PBS for three times. After cleaning, the surfaces were incubated in 300 µl of 1% sodium dodecyl sulfate (SDS) solution for 4 hours. The surface exposed SDS solution with the adsorbed protein was then used with a Micro-BCA assay to measure the absorbance using a plate reader. The protocol provided by the manufacturer was followed to obtain absorbance and to plot the standard curve. The actual protein concentrations were calculated and normalized with the area of the surface.

The surfaces exposed to proteins were also characterized using XPS. The surface chemistry was analyzed using the XPS survey scans by detecting the presence of nitrogen (N1s) on each surface. Protein adsorption is directly proportional to the amount of nitrogen present on the surfaces and is a very accurate representation of protein adsorption.

3.2.3 Statistical analysis

Every analysis was carried out in repetitions of at least three times to find their mean and variability. Exposure to proteins (fibrinogen and albumin) in both static and dynamic conditions were repeated at least three times with three different samples of each kind every time ($n_{min} = 9$). Protein adsorption was measured using BCA Assay and by surface characterization using XPS by measuring the amount of nitrogen present on each surface. The results were analysed using a software JMP Pro to find ANOVA and student's t test. Statistical significance was calculated using JMP Pro using a 0.95 probability of occurrence.

3.3 Protein adsorption on different surfaces

3.3.1. Micro-BCA assay:

Protein adsorption on the different surfaces was characterized using a micro-BCA assay in both static and dynamic conditions. Protein adsorption on a surface is characteristic of its hemocompatibility. As blood makes contact with the external surface, plasma proteins start adsorbing to the surface. Fibrinogen and Albumin are the two main proteins in blood which are present in abundance in blood and actively adsorb on external surfaces. Their adsorption depends on the surface properties they such as chemistry, topography and energy. In the presence of fibrinogen, which is a pro-coagulant protein, platelets adhere to the surfaces and to each other resulting in platelet activation. This eventually leads to thrombin formation as more cells tend to adhere to the activated platelets creating clots. On the contrary, presence of Albumin may lead to less clotting of blood as Albumin acts as a passivating protein, however this is not the only reason why blood will not clot. In this study, Fibrinogen and Albumin adsorption was investigated as fibrinogen has a key role in starting the process of thrombosis and albumin is the most abundant protein present in our blood.

In static studies, both the proteins showed similar trends for all the surfaces. In case of Fibrinogen, Ti-S and NT-S had the least adsorption since the surfaces are hydrophobic in nature (**Figure 3.3.1B**). Although Ti-S and NT-S had different protein adsorption values, they showed similar trends of low adsorption as protein adsorption majorly depends on hydrophobicity along with other factors like surface characteristics and the size and shape of the proteins. On the contrary, NT-PEG had the highest adsorption when compared to all the other surfaces as the surface is hydrophilic and the hydrophilic surfaces interact better with proteins. The fibrinogen adsorption on NT-S and NT-PEG was significantly different from each other (**Figure 3.3.1B**). Similarly, in case of Albumin, Ti-S and NT-S had the least adsorption, whereas, Ti-PEG had the highest adsorption when compared to all the other surfaces. The albumin adsorption on Ti-S and Ti-PEG was significantly different from each other (**Figure 3.3.1A**).

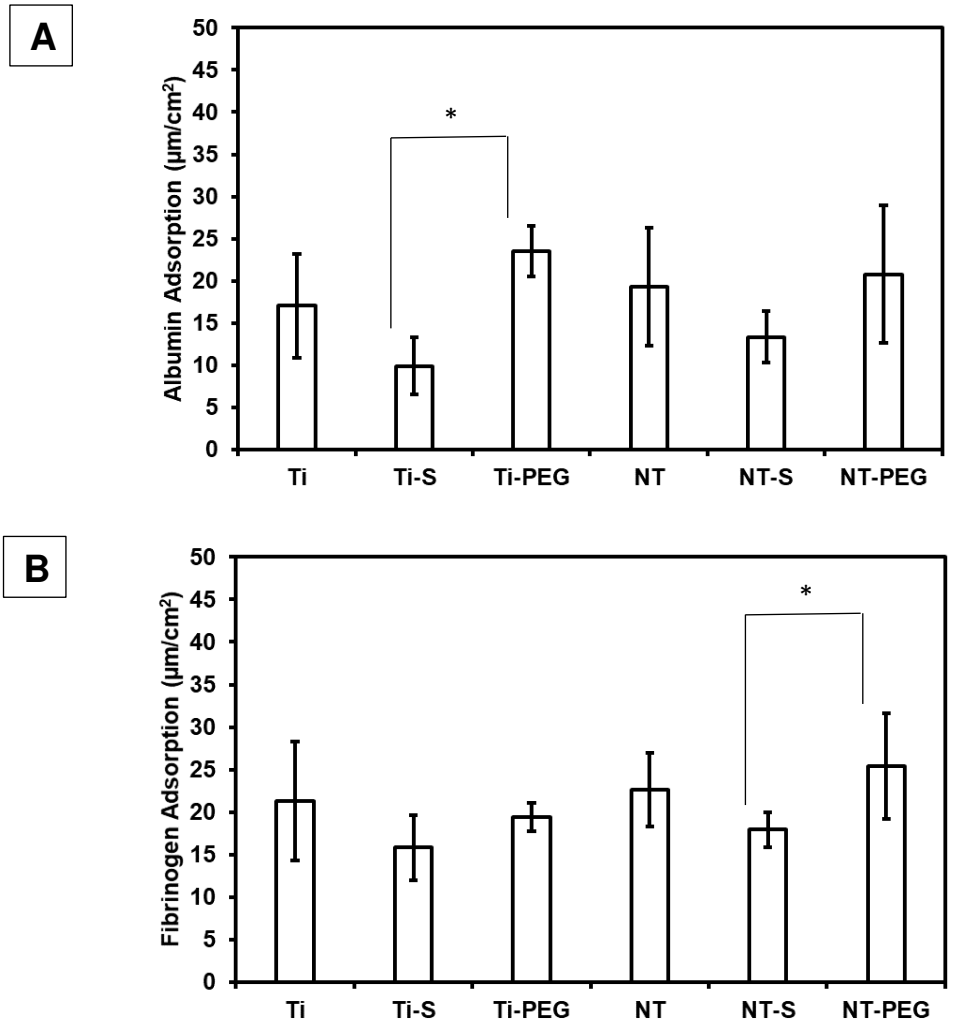

Figure 3.3.1: (A) Static albumin binding on different surfaces. Statistical differences in albumin adsorption between Ti-S and Ti-PEG ($p < 0.05$) (B) Static Fibrinogen binding on different surfaces. Statistical differences in fibrinogen adsorption between NT-S and NT-PEG ($p < 0.05$)

In dynamic studies, both proteins showed similar trends on all the surfaces. In case of Fibrinogen, Ti-S showed the least protein adsorption followed by NT-S. NT-PEG showed the highest protein adsorption of all samples. NT-PEG showed statistical significance to NT-S. In between NT-S and Ti-S, the latter performed significantly better as the results indicated a significance between the two with Ti-S showing lesser adsorption rates (**Figure 3.3.2B**). For Albumin, NT-S showed the least adsorption rates amongst all samples followed by Ti-S. Similar to previous results, NT-PEG showed the highest protein adsorption rate. Although there is no

statistical significance between the samples, the graphs as shown in **Figure 3.3.2A** clearly show that NT-S performs the best in this case.

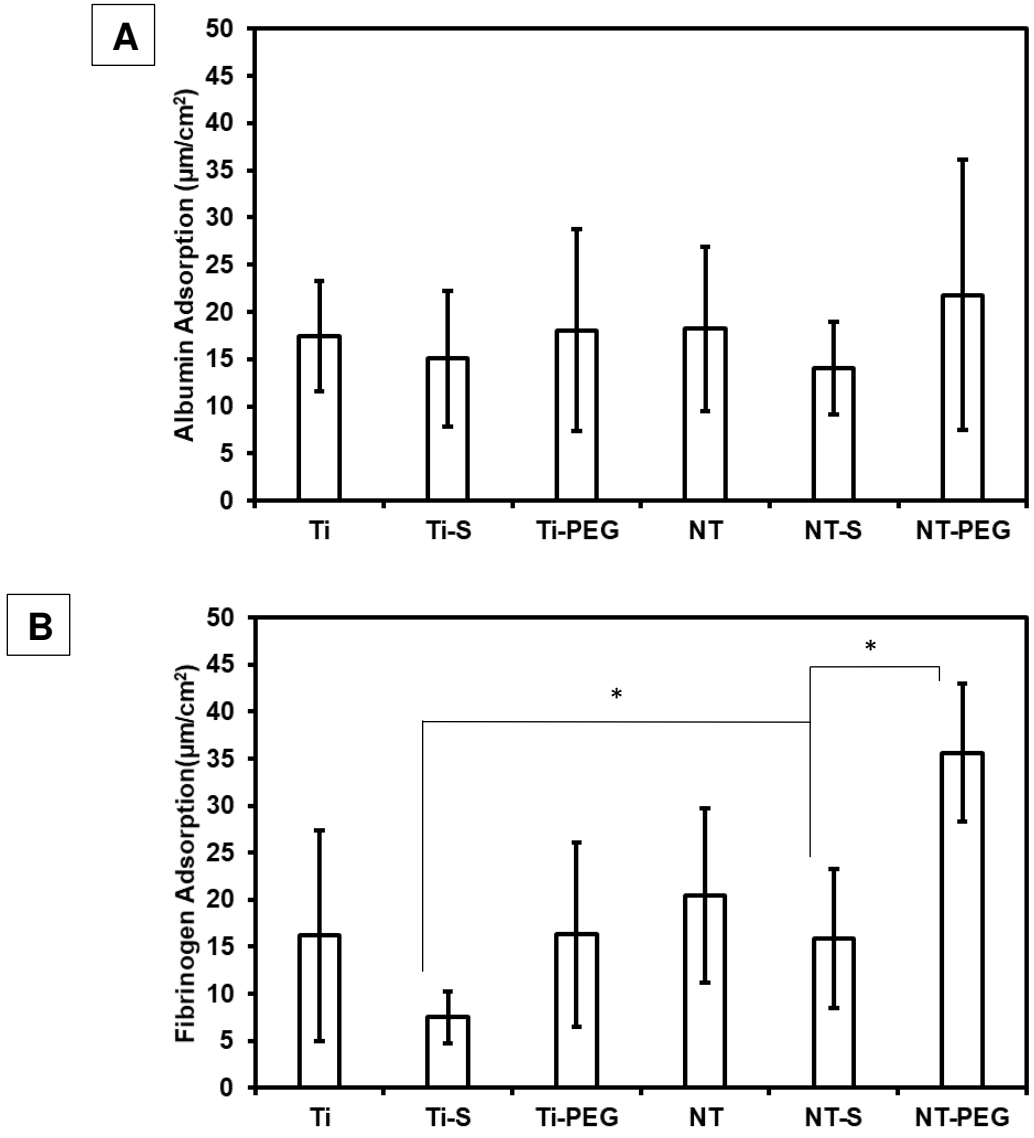

Figure 3.3.2: (A) Dynamic albumin binding on different surfaces. (B) Dynamic Fibrinogen binding on different surfaces. Statistical differences in fibrinogen adsorption between NT-S and NT-PEG ($p < 0.05$) and between NT-S and Ti-S ($p < 0.05$)

The results of static and dynamic protein adsorption were compared for each surface to evaluate if there is any difference. The results of Fibrinogen adsorption indicated all surfaces showed lower amounts of protein adsorption in dynamic studies when compared to static studies except for NT-PEG (**Figure 3.3.3B**). Only NT-PEG showed an increase in protein adsorption for

dynamic studies that was statistically significant (**Figure 3.3.3B**). This might be because the affinity of the surfaces towards proteins increases due to the presence of PEG and due to the presence of NT over the base surfaces might have created a greater obstruction to the already constricted flow of plasma through the dynamic chamber resulting in more protein adsorption. The results for Albumin in both static and dynamic adsorption showed similar values. Ti-PEG showed a lower adsorption rate in dynamic compared to static whereas Ti-S showed more adsorption in dynamic compared to static (**Figure 3.3.3A**). None of the samples showed significant changes in static and dynamic results.

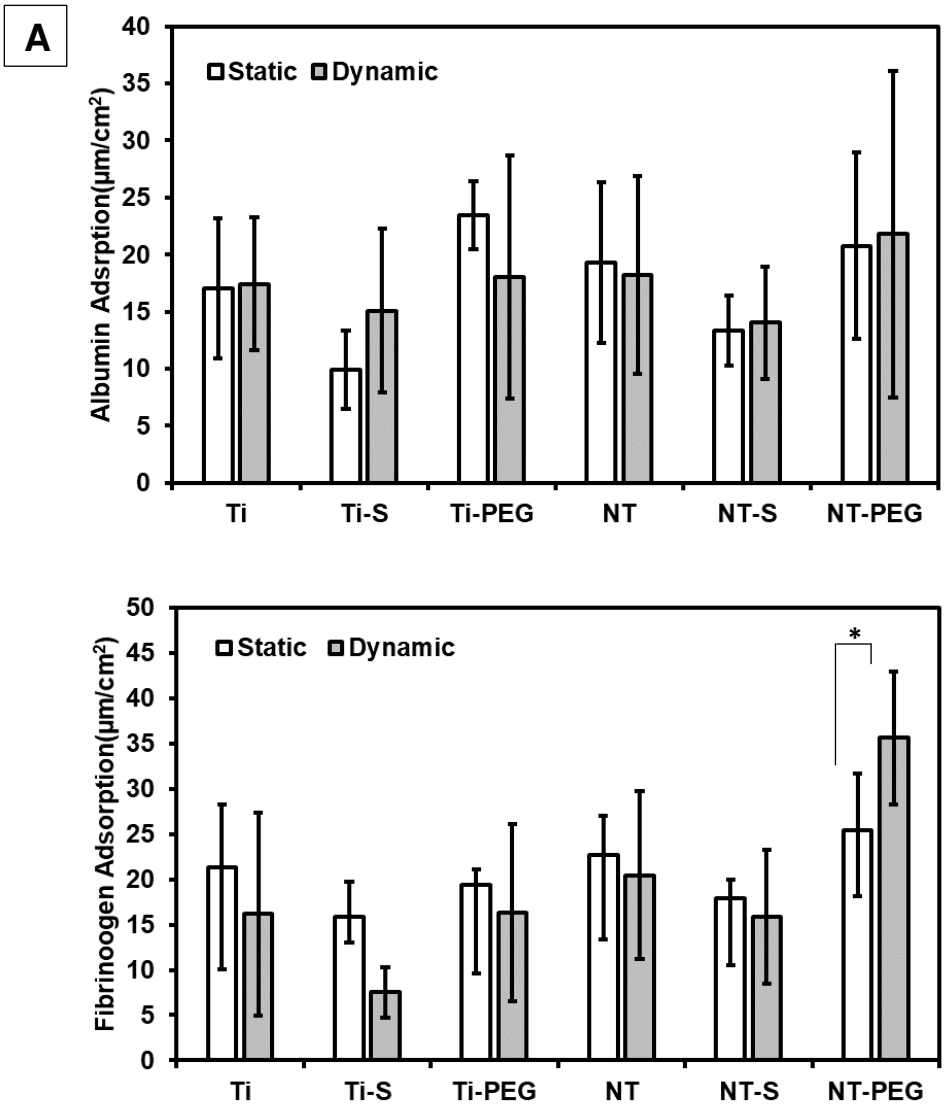

Figure 3.3.3: (A) Albumin binding on different surfaces after static and dynamic albumin exposure. (B) Fibrinogen binding on different surfaces after static and dynamic fibrinogen exposure. Statistical differences in fibrinogen adsorption between static and dynamic for NT-PEG ($p < 0.05$)

3.3.2. XPS for surface nitrogen concentration

Protein adsorption was also characterized using XPS by comparing the nitrogen (N1s) peak on all the surfaces. BCA assay is a quick methodology to obtain protein adsorption values but not the most accurate whereas, XPS is a very accurate elemental analysis of the surfaces. N1s peaks were compared since only proteins consisted of nitrogen and XPS would give an accurate representation of the presence of elemental N1s on the surface. The results obtained from micro-BCA assay and XPS differed in some cases. For static studies, albumin and fibrinogen both showed similar trends. For Fibrinogen, NT-S has the smallest the least presence of nitrogen concentration followed by the other samples. On the contrary, NT and NT-PEG showed the highest nitrogen concentration. For Albumin, NT-S showed the least protein adsorption followed by Ti-S. NT and NT-PEG showed the highest adsoption of protein. In contrary to the results obtained from the BCA assay, NT-S performed the best amongst all surfaces as it had the least presence of nitrogen concentration on the surface. Since XPS is a much reliable method of studying protein adsorption, we can assertively conclude that NT-S showed the lowest protein adsorption in static condition.

A

Fibrinogen Static XPS

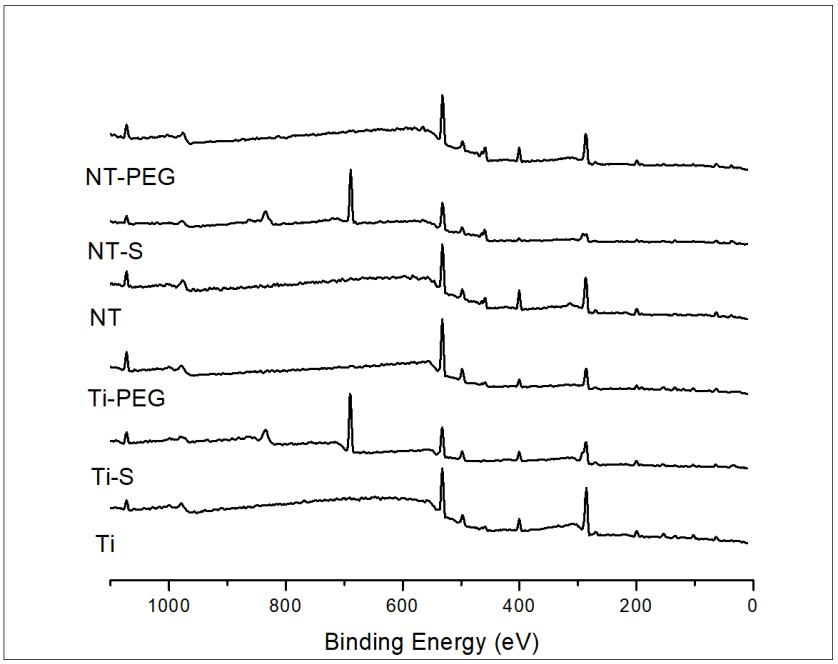

B

Albumin Static XPS

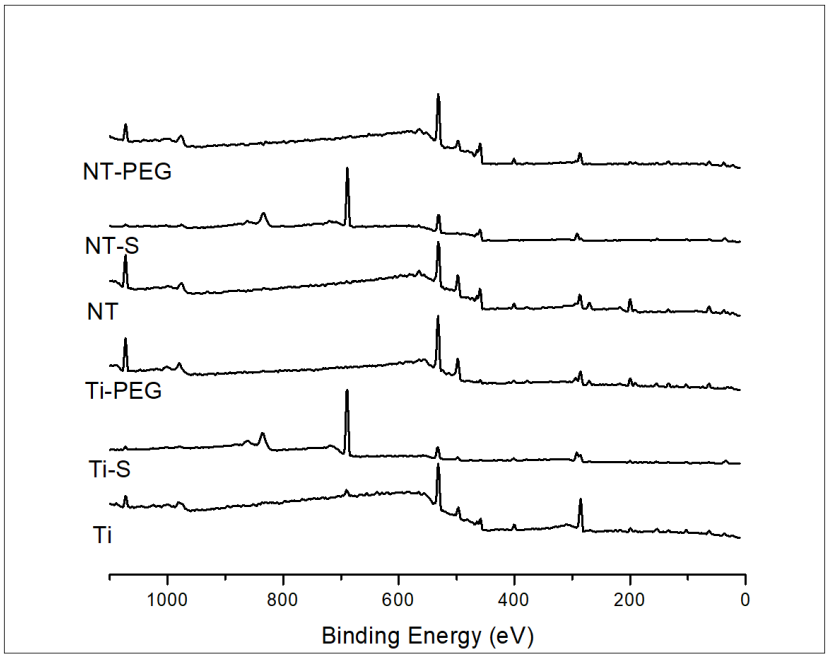

Fig 3.3.4: Representative XPS survey scans for (A) Static fibrinogen study and (B) Static albumin study.

Dynamic protein adsorption was similar to static results although the hydrophobic samples showed much lesser adsorption rates compared to the static study. The results of Fibrinogen indicated NT-S was the surface that adsorbed the least protein followed by Ti-S. NT-PEG showed the highest protein adsorption rate of all the samples. Albumin results indicated NT-S and Ti-S showed lowest hemocompatibility. Ti-PEG also showed very low adsorption rates followed by the other surfaces. NT-PEG showed the highest adsorption among all the surfaces.

A

Fibrinogen Dynamic XPS

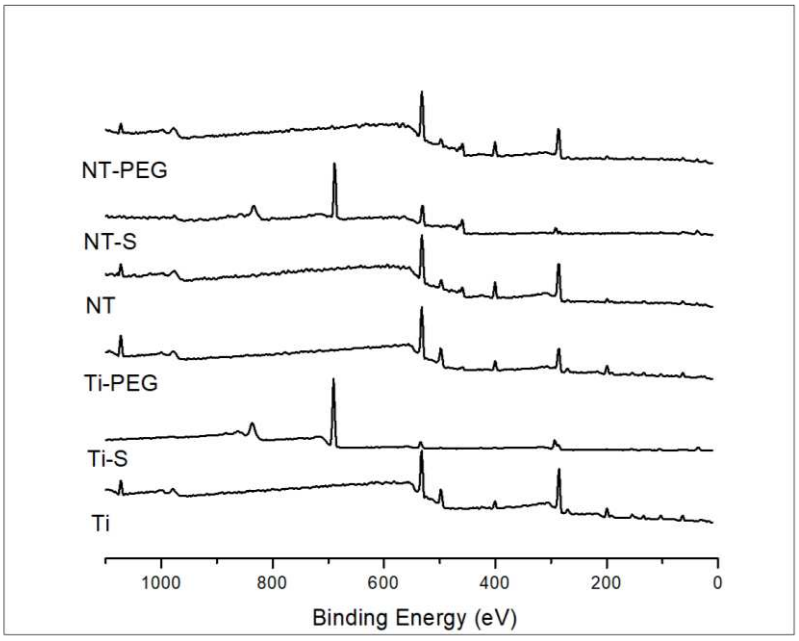

B

Albumin Dynamic XPS

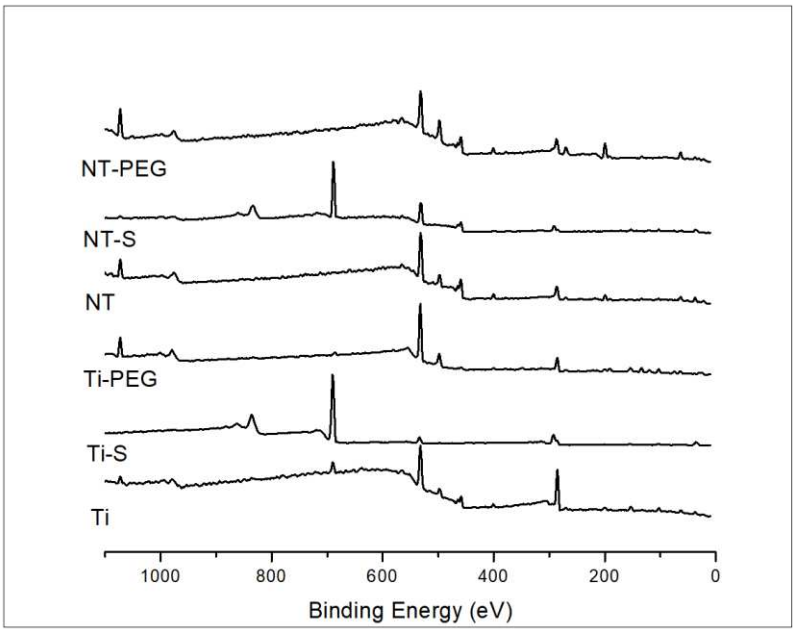

Fig 3.3.5: Representative XPS survey scans for (A) Dynamic fibrinogen study and (B) Dynamic albumin study.

Comparing the static and dynamic results for each protein, it was observed that for albumin, all surfaces showed lower protein adsorption in dynamic conditions except NT-S, which showed very low protein adsorption in both cases (**Table 3.3.1A**). For Fibrinogen, NT-S showed a decrease in protein adsorption in dynamic conditions with a value close to zero which signified no protein adsorption. Ti-PEG, NT-PEG showed higher protein adsorption in dynamic conditions and although NT also showed a slight increase in dynamic conditions, the results were comparable (**Table 3.3.1B**). Both proteins, Fibrinogen and Albumin showed a difference in adsorption rates in dynamic conditions compared to static, proving that there is a change in protein interaction between static and dynamic conditions. Dynamic protein adsorption is lower than static protein adsorption in most cases since in case of dynamic, the proteins are in constant motion whereas in static conditions the proteins are stagnant over the surface making them more susceptible to protein adsorption.

Table 3.3.1: (A) Adsorption percentages of different materials on the surfaces after static (S) and dynamic (D) exposure to human albumin. (B) Adsorption percentages of different materials on the surfaces after static (S) and dynamic (D) exposure to human fibrinogen.

A

Albumin Static/Dynamic

	O1s		F1s		Si2p		Cl2p		Ti2p		C1s		N1s	
	S	D	S	D	S	D	S	D	S	D	S	D	S	D
Ti	35.46	31.15	0	0	0	0	0	0	3.15	3.12	56.61	62.9	4.77	2.83
Ti-S	11.93	6.92	47.82	57.79	3.24	3.6	0.82	0.48	0.3	0	33.21	30.41	2.68	0.81
Ti-PEG	52.25	55.73	0.29	1.87	5.75	7.86	4.24	0	0.88	0.94	33.74	31.82	2.84	1.78
NT	48.65	50.2	0	0	0	0	0	0	7.4	7.8	37.13	36.4	6.81	5.7
NT-S	20.99	25.5	48.76	44.6	2.13	4.2	0.01	0.2	4.95	4.5	22.76	20.1	0.4	0.6
NT-PEG	53.3	41.0	1.36	0.9	2.27	1.6	0.73	6.2	8.36	5.9	28.01	37.8	5.97	6.5

B

Fibrinogen Static/Dynamic

	O1s		F1s		Si2p		Cl2p		Ti2p		C1s		N1s	
	S	D	S	D	S	D	S	D	S	D	S	D	S	D
Ti	26.84	29.85	0	0	0	0	0	0	1.02	0.03	63.59	65	8.55	5.12
Ti-S	18.44	7.47	26.47	56.32	1.73	3.7	1.88	0.53	0.18	0.24	44.03	30.22	7.27	1.52
Ti-PEG	43.82	38.01	1.58	0.12	4.18	2.95	0.95	3.41	1.43	0.93	41.22	45.29	6.82	9.3
NT	29.34	28.42	0	0	0	0	0	0	2.22	2.21	55.18	58.26	10.26	11.1
NT-S	25.75	24.59	34.46	46.35	1.82	3.57	0.64	0.14	4.16	6.73	30.47	18.62	2.71	0
NT-PEG	31.51	31.23	1.65	0.38	1.03	1.71	1.71	0.46	3.52	3.05	49.79	51.09	10.78	12.07

3.4 Conclusion

The results obtained from protein adsorption indicated higher hemocompatibility for silane coated surfaces since they showed lower protein adhesion for both proteiins in static and dynamic conditions. The dynamic and static protein adsorption resylts were different from each other and dynamic results showed lower protein adhesion to static results but the trends shown in both conditions were the same. NT-S was the surface that performed the best overall for both proteins.

REFERENCES

1. Kasemo B. Biological surface science. Surface Science. 2002 Mar 10;500(1–3):656–77.
2. Carré A, Lacarrière V. How substrate properties control cell adhesion. A physical-chemical approach. Journal of Adhesion Science and Technology. 2010 Apr 1;24(5):815–30.
3. Parhi P, Golas A, Vogler EA. Role of proteins and water in the initial attachment of mammalian cells to biomedical surfaces: A review. Journal of Adhesion Science and Technology. 2010 Apr 1;24(5):853–88.
4. (No Title) [Internet]. [cited 2020 Oct 7]. Available from: http://www.terumo-cvgroup.com/doc/Schiel_CanadianPerfusionCanadienne_11_No2.pdf

CHAPTER 4

CELL ADHESION ON TITANIA NANOTUBE SURFACES IN STATIC AND DYNAMIC CONDITIONS

4.1. Introduction

Protein adsorption on the surfaces drives the subsequent integration of the materials with cells as the adsorbed proteins act as the mediators between the surface properties of the material and the cell receptors(1–7). Platelet adhesion and activation is a leading factor in thrombin formation(8). Platelets, in the presence of proteins adhere to the surfaces and get activated and in turn activates other platelets in contact with them. The lesser the adhered cells on the surface, the better the hemocompatibiity for the surface. Thus in this study the surfaces were exposed to PRP both in static and dynamic conditions and were investigated under a fluorescence microscope. Calcein-AM, Rhodamine phalloidin and DAPI were the three stains used to stain the cells. Platelet activation was investigated under the SEM for all surfaces.

4.2. Materials and Methods

4.2.1. Static vs. dynamic studies on different surfaces

Static studies were done by incubating the surfaces in a 48-well plate with 300 µl fluid (Tyrode solution, protein solution, platelet rich plasma (PRP)) for 2 hours on a shaker at 100 rpm inside an incubator with fixed conditions of 37°C and 5% CO_2. The surfaces were then cleaned with PBS three times and characterized as discussed below.

Dynamic studies were done by placing the substrates inside the flow chamber and flowing fluid (Tyrode solution/protein solution/platelet rich plasma) through the flow chamber at a constant rate of 20 ml/hr for 30 minutes for each sample inside the bio-hood. The surfaces were then cleaned with PBS three times and characterized as discussed below.

4.2.2. PRP (platelet rich plasma) isolation from whole blood

PRP was obtained from whole blood from healthy donors who weren't on any medication that may have affected their blood and its contents. Whole blood was collected through venipuncture in 6ml EDTA (ethylenediaminetetraacetic acid) tubes and the procedure was in compliance with the National Institutes of Health's "Guiding Principles for Ethical Research" and approved by Colorado State University Institutional Review Board. The blood was then centrifuged at 150 g for 15 minutes to separate the different layers of blood. The PRP was pooled prior to exposing it on the surfaces. Surfaces were sterilized prior to static and dynamic studies using 70% ethanol for 15 minutes. After 15 minutes, the ethanol was aspirated and the surfaces were washed with PBS three times and used for either static of dynamic studies.

4.2.3. Cell adhesion on different surfaces

The cell adhesion on all the surfaces was characterized by staining the live cells with a calcein-AM working solution and visualizing the surfaces under fluorescence microscope. The surfaces exposed to PRP in static and dynamic conditions were incubated with 300 µl of 5% calcein-AM solution for 20 minutes inside a dark room. After that, the calcein-AM solution was aspirated, and the substrate was washed three times with PBS before taking them for imaging using fluorescence microscopy. Images were taken at a magnification of 10X and 20X on the substrates. To measure the surface coverage of live cells, the images were processed with Image J.

4.2.4. Platelets and leukocytes identification on different surfaces

Identification of platelets and leukocytes adhered on surfaces was done by staining the cells with DAPI (4', 6 – diamidino – 2 – phenylindole) and rhodamine phalloidin (actin) and visualized under a fluorescence microscope. Platelets lack nuclei thus will not be stained by DAPI, whereas all cells will be stained by rhodamine phalloidin since they have cytoskeleton. The

substrates were incubated in 300 µl of 3.7% formaldehyde solution for 15 minutes (for fixation). After this the surfaces were incubated in PBS for 5 minutes, twice before incubating it in 1% Triton solution for 3 minutes. The surfaces were incubated four times in PBS for 5 minutes each time. After aspirating the PBS, the surfaces were stained with 200 µl of 0.05% rhodamine phalloidin solution for 25 minutes followed by adding 21 µl of 3% stock DAPI solution on top of rhodamine for an additional 5 minutes. After aspiring the stain solution, the substrates were imaged using fluorescence microscopy at a magnification of 20X. The red stains represented the platelets and leukocytes, whereas the blue stains represented just leukocytes. To measure the surface coverage of live cells, the images were processed with Image J.

4.2.5. Platelet activation on different surfaces

Platelet activation was visualized on each surfaces using a SEM. After aspirating the PBS, the platelets on the substrates were fixed by incubating them in a primary fixative solution (6% glutaraldehyde, 0.1M sodium cacodylate and 0.1M sucrose in DI water) for 45 minutes. Then they are transferred to a buffer solution (0.1M sodium cacodylate and 0.1M sucrose for 10 mins) for 10 minutes. Then the substrates were incubated in increasing concentrations of ethanol for 10 minutes each, starting from 35%, 50%, 70% and finally to 100% ethanol. The substrates were let to dry inside the biosafety cabinet and were imaged using SEM at magnifications of 500X, 2000X and 10000X. The surfaces were coated with gold with a 5 nm thickness prior to imaging to protect the platelets from disintegrating.

4.2.6. Statistical analysis

Every analysis was carried out in repetitions of at least three times to find their mean and variability. Surface characterization was done on at least three different places on a surface. SEM images were taken at least on three different locations on each surface. Exposure to PRP in both static and dynamic conditions were repeated at least three times with three different samples of

each kind every time (n_{min} = 9). Fluorescence images on a sample were taken at least three different spots for all stains (Calcein-AM, Rhodamine phalloidin, DAPI) The results were analysed using a software JMP Pro to find ANOVA and student's t test. Statistical significance was calculated using JMP Pro using a 0.95 probability of occurrence.

4.3. Results and Discussion

4.3.1. Cell Adhesion on different surfaces

Cell adhesion of platelets and leukocytes on the surfaces was characterized using a fluorescence microscope. Cell adhesion reflects protein denaturation and cell reactivity on the surface. These adhered cells may form clots and lead to thrombosis. The lesser the adhered cells on the surface indicates better hemocompatibility of the surface. The adhered cells were stained with Calcein-AM, Rhodamine phalloidin and DAPI stains and the images where processed with ImageJ to get cell counts and percent area coverage. Platelet and leukocyte adhesion and aggregation on different surfaces impact the production of anticoagulant molecules which hinder the resistance to thrombosis. In the presence of proteins, cells adhere to the surface and activate, thus it is important to study the adhesion and aggravation of cells on the surfaces. Initially, to evaluate cell adhesion, Calcein-AM was used which stains the cytoplasm of the live cell green in fluorescence microscope.

In static study, NT-S and NT-PEG showed the least cell adhesion. In general, the surfaces with nanostructures showed lower cell adhesion than titanium as the platelets had lower surface area to attach to which allowed the cells to glide on the surface rather than getting attached and activating (**Figure 4.3.1A**). Cell adhesion results in Ti and NT were significantly different from each other as was the case for Ti-S and NT-S. In case of NT-S and NT-PEG, the modifications created a surface that made it surfaces even more hemocompatible. Ti showed the highest cell adhesion as the hydrophilic surface without the presence of nanostructures made the surfaces

susceptible to cell adhesion. Ti was significantly different from Ti-PEG, which showed lower cell adhesion than Ti (**Figure 4.3.1B**).

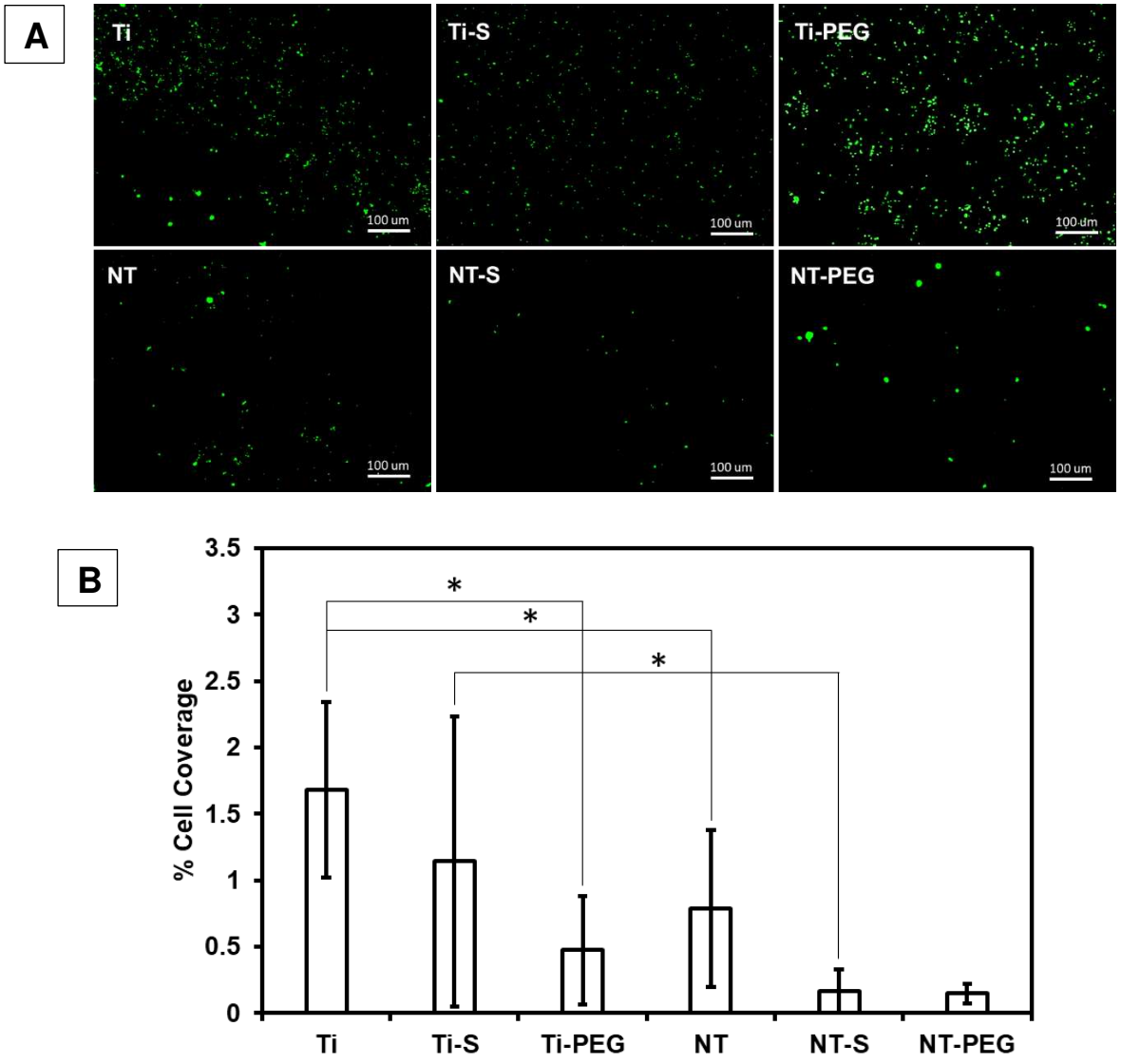

Figure 4.3.1: (A) Fluorescence microscopy images of different surfaces stained with Calcein-AM after static human platelet exposure from PRP. (B) Percent area coverage of cells on different surfaces. Statistical differences in percent area coverage of cells between Ti and Ti-PEG, Ti and NT, Ti-S and NT-S ($p < 0.05$).

In dynamic study, the trend for cell adhesion was very similar to that of static study. Surfaces modified with nanostructures showed lower cell adhesion than unmodified surfaces. NT showed the lowest cell adhesion compared to all other surfaces followed by NT-S. Ti-PEG showed

the highest protein adsorption (**Figure 4.3.2A & 4.3.2B**). In case of dynamic studies, the coating on the nanostructures might have hindered the lateral flow of cells over the surfaces which led to higher cell adhesion and the presence of nanostructures as the primary structures could have assisted to the lower cell adhesion than the unmodified Ti surface.

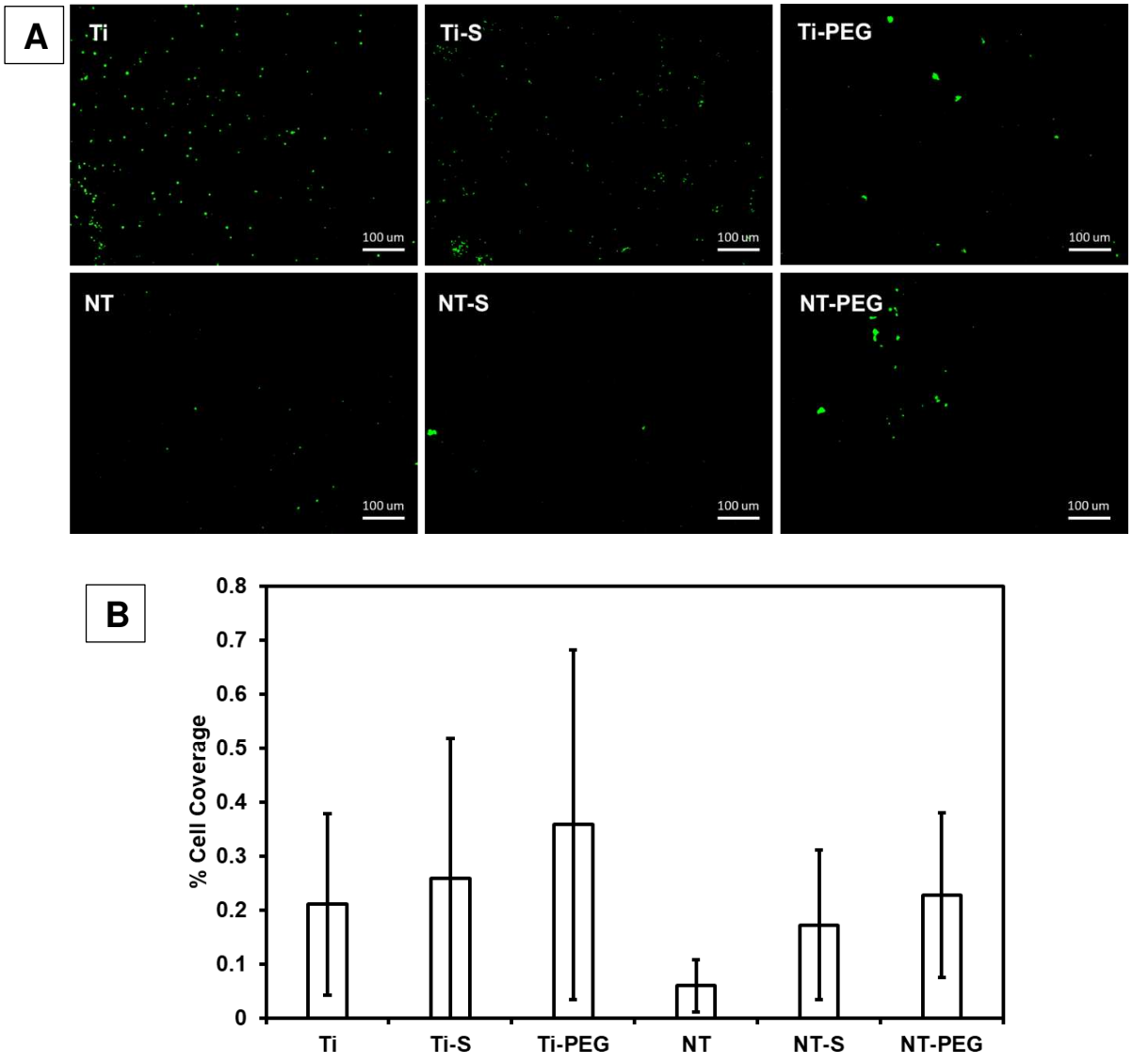

Figure 4.3.2: (A) Fluorescence microscopy images of different surfaces stained with Calcein-AM after dynamic human platelet exposure from PRP. (B) Percent area coverage of cells on different surfaces.

Since Calcein-AM stained all cells i.e. both platelets and leukocytes, it is impossible to differentiate between these cells. Hence, Rhodamine phalloidin and DAPI were used to stain the

cells on the surface. Rhodamine stains cytoskeleton of the cells red, whereas DAPI stains nucleus of the cells blue in fluorescence microscopy. Thus, Rhodamine phalloidin and DAPI will allow to differentiate platelets and leukocytes adhered on the surface since platelets and leucocytes both will stain for Rhodamine phalloidin since both have cytoskeleton, whereas, only leukocytes will stain for DAPI as platelets do not have nucleus.

In static studies, the trend for cell adhesion was very similar to that of cell adhesion results. NT and NT-S showed the least adhesion of platelets and leukocytes. Ti-PEG and NT-PEG had the highest cell adhesion compared to all other surfaces. NT-PEG showed significantly higher cell adhesion than NT and NT-S. Similarly, Ti-PEG showed significantly higher cell adhesion than Ti-S (**Figure 4.3.3A & 4.3.3B**). In DAPI static studies, the results indicated NT as the surface with the lowest leukocyte adhesion. Ti-PEG had the highest adhesion because of the hydrophilic coating on a non-textured surface which increased its affinity towards protein adsorption and cell adhesion (**Figure 4.3.3A & 4.3.3C**).

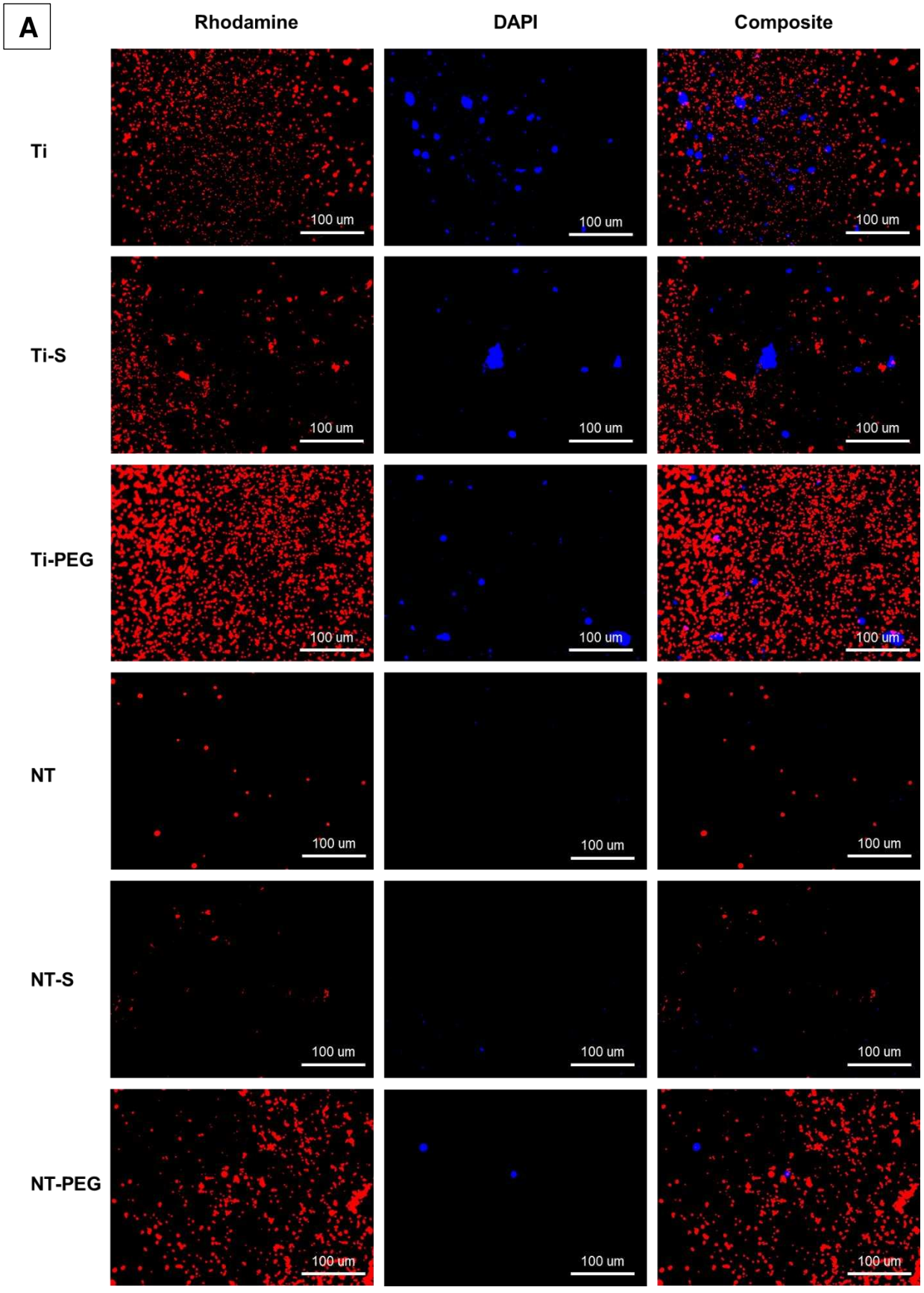
A
Rhodamine
DAPI
Composite
Ti
Ti-S
Ti-PEG
NT
NT-S
NT-PEG
100 um

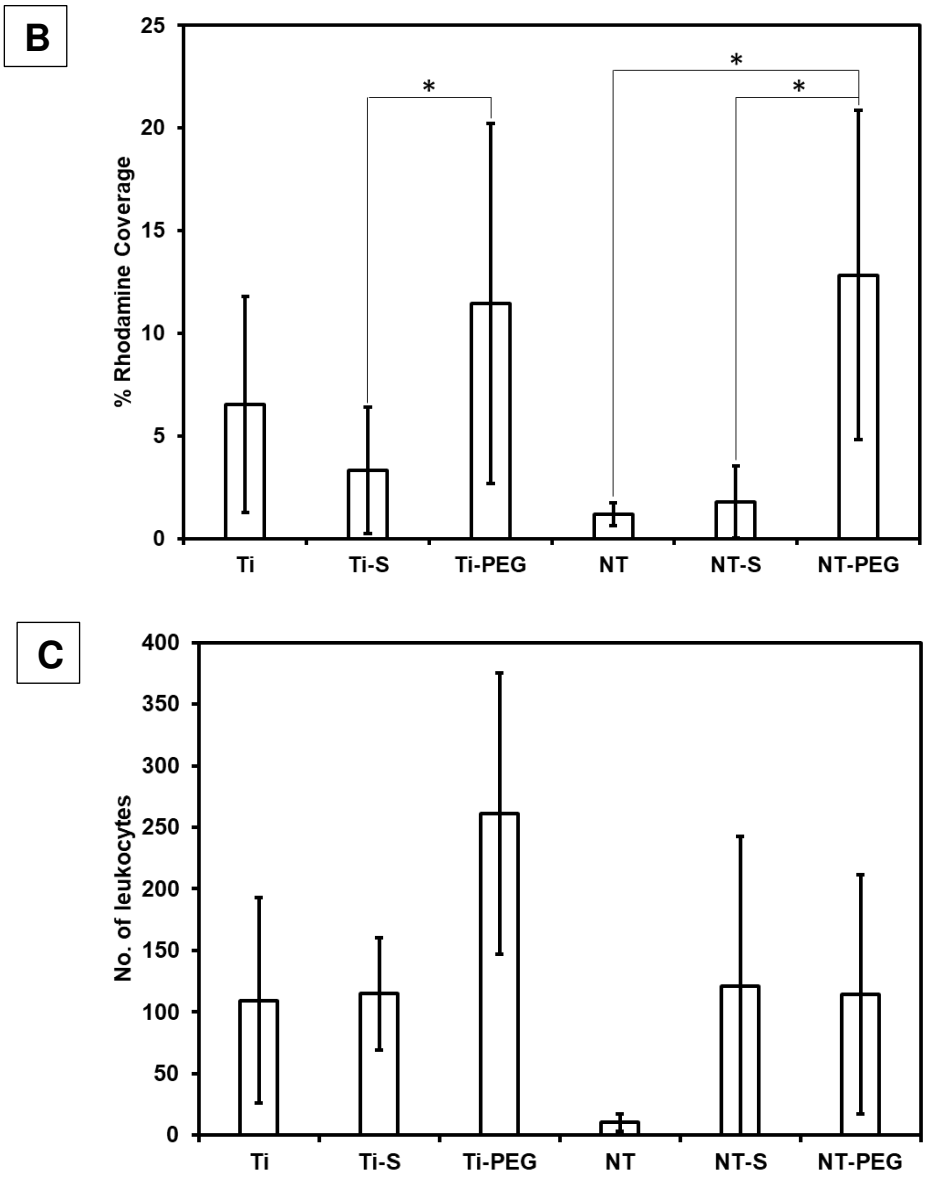

Figure 4.3.3: (A) Fluorescence microscopy images of different surfaces stained with DAPI (blue) and Rhodamine phalloidin (red) after static human platelet exposure from PRP. (B) Percent area coverage of cells on different surfaces. Statistical differences in percent are coverage of cells between Ti-S and Ti-PEG, NT and NT-PEG, NT-S and NT-PEG ($p < 0.05$) (C) Number of adhered leukocytes on different surfaces.

In dynamic studies, NT-S showed the lowest cell adhesion which was negligible followed by Ti-S. Ti had the highest cell adhesion of all the surfaces followed by NT-PEG. Ti showed significantly higher cell adhesion over Ti-S and Ti-PEG. NT also had a significantly lower cell adhesion than Ti (**Figure 4.3.4A & 4.3.4B**). DAPI dynamic studies showed very similar trends to

that of Rhodamine dynamic where surfaces with nanostructures showed significantly less cell adhesion than the non-textured surfaces. NT-S showed least adhesion whereas Ti had the highest cell adhesion among all the surfaces (**Figure 4.3.4A & 4.3.4C**).

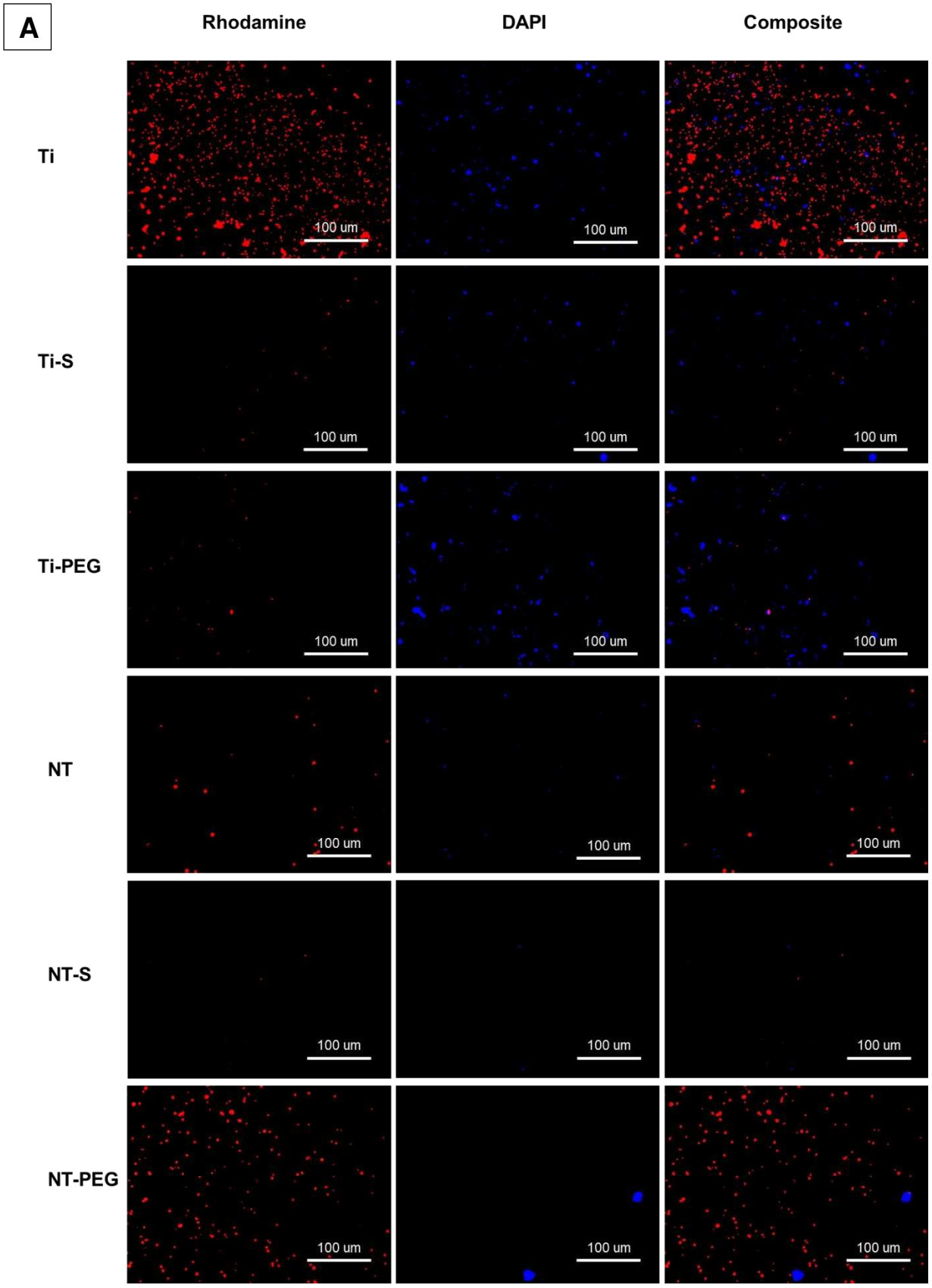
A
Rhodamine
DAPI
Composite
Ti
Ti-S
Ti-PEG
NT
NT-S
NT-PEG
100 um

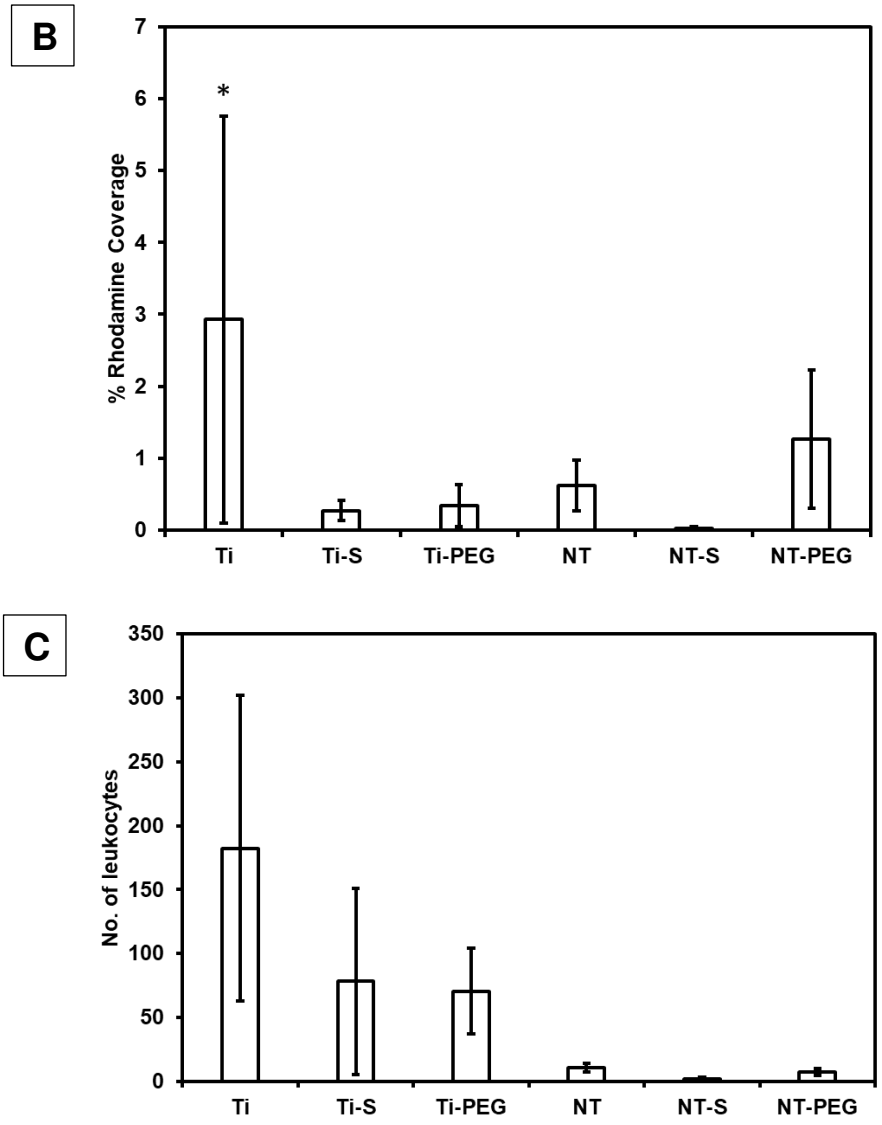

Figure 4.3.4: (A) Fluorescence microscopy images of different surfaces stained with DAPI (blue) and Rhodamine phalloidin (red) after dynamic human platelet exposure from PRP. (B) Percent area coverage of cells on different surfaces. Statistical differences in percent area coverage of cells between Ti and all other surfaces (C) Number of adhered leukocytes on different surfaces.

4.3.2. Platelet adhesion and activation

Platelet adhesion and activation was visualized using SEM. Activated platelets show filopodial extensions which look like small tendrils coming out of the platelet body. On further activation, the platelets show lamellipodial extensions ultimately resulting in the complete disintegration of the platelets onto the surface. During the activation procedure, the platelets

instigate leukocyte localization and this leukocyte-platelet interaction may lead to thrombosis. For this reason, the SEM images are particularly important to investigate the extent of activation of the platelets. The SEM Images were taken after both static and dynamic platelet exposure.

In static conditions, NT-S showed the least platelet adhesion. On the other hand, Ti showed the highest platelet adhesion which was in line with the previous results from fluorescence microscopy (**Figure 4.3.5**). Platelet activation was also analyzed from the SEM images and none of the surfaces showed signs of platelet activation. Ti showed signs of platelet denaturation but no clear signs of activation could be identified.

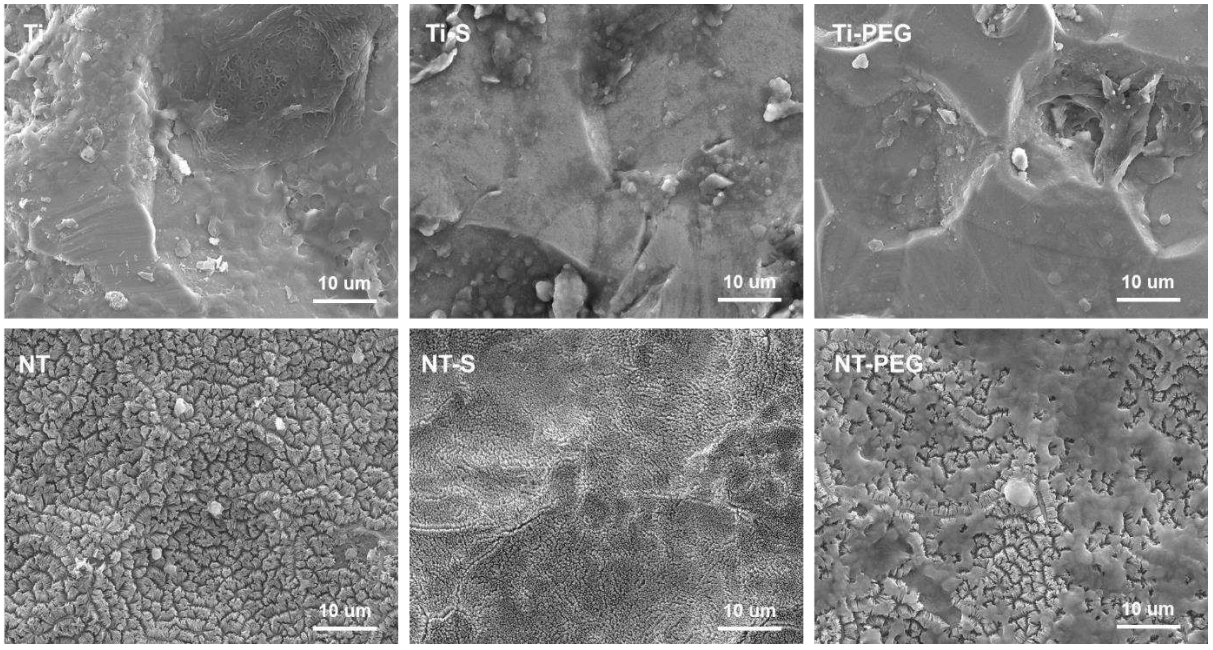

Figure 4.3.5: Representative SEM images of surfaces after static human platelet exposure from PRP.

In Dynamic conditions, the NT surfaces showed close to no platelet adhesion with NT-S showing the least platelet adhesion among all the surfaces. Ti showed the highest platelet adhesion (**Figure 4.3.6**). Platelet activation was also analysed after dynamic platelet exposure and similar to static results did not show any sign of platelet activation.

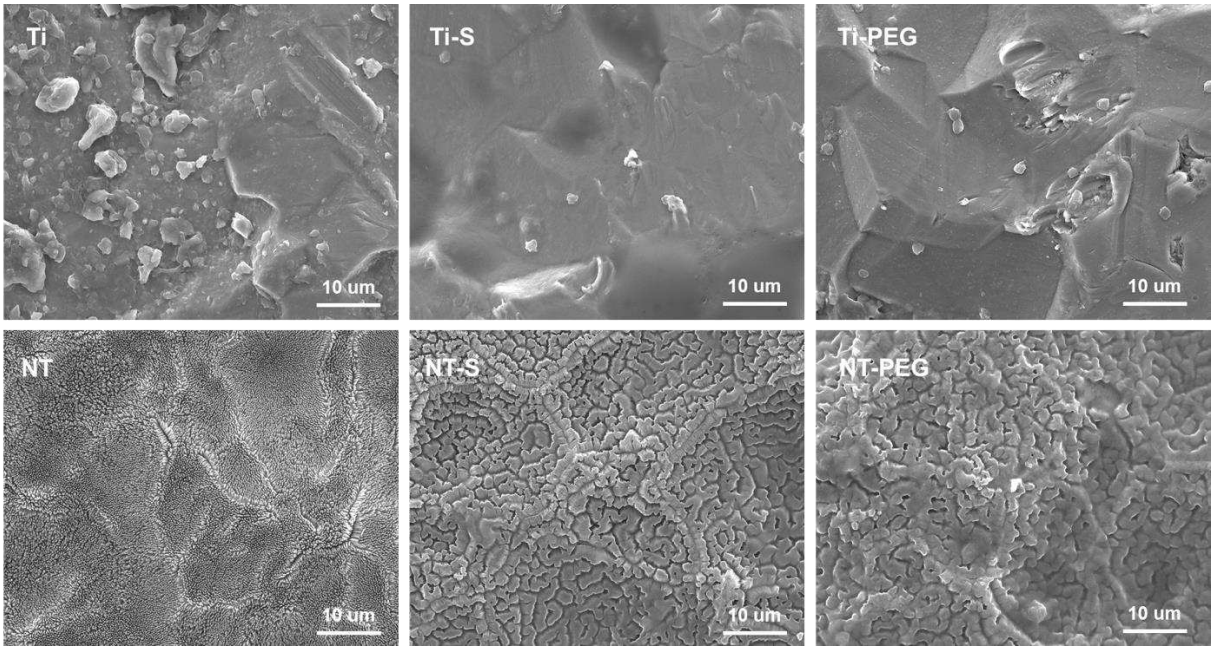

Figure 4.3.6: Representative SEM images of surfaces after dynamic human platelet exposure from PRP.

4.4 Conclusion

The results obtained from the cell studies indicated that NT surfaces adhered lower cells in general in both static and dynamic conditions over titanium surfaces. NT-S was the best performing material and showed the highest hemocompatibility. The SEM results reflected the same trend and it also showed there was no clear sign of cell activation on any of the surfaces.

REFERENCES

1. Kasemo B. Biological surface science. Surface Science. 2002 Mar 10;500(1–3):656–77.
2. Carré A, Lacarrière V. How substrate properties control cell adhesion. A physical-chemical approach. Journal of Adhesion Science and Technology. 2010 Apr 1;24(5):815–30.
3. Parhi P, Golas A, Vogler EA. Role of proteins and water in the initial attachment of mammalian cells to biomedical surfaces: A review. Journal of Adhesion Science and Technology. 2010 Apr 1;24(5):853–88.
4. Scopus - Document details [Internet]. [cited 2020 Oct 7]. Available from: https://www.scopus.com/record/display.uri?eid=2-s2.0-84935420977&origin=inward&txGid=fd115d1e1f572532a2a7c2904ef04436
5. Tsapikouni TS, Missirlis YF. Protein-material interactions: From micro-to-nano scale. Vol. 152, Materials Science and Engineering B: Solid-State Materials for Advanced Technology. 2008. p. 2–7.
6. Ponche A, Ploux L, Anselme K. Protein/material interfaces: Investigation on model surfaces. Journal of Adhesion Science and Technology. 2010 Sep 1;24(13–14):2141–64.
7. Silva-Bermudez P, Rodil SE. An overview of protein adsorption on metal oxide coatings for biomedical implants. Vol. 233, Surface and Coatings Technology. Elsevier; 2013. p. 147–58.
8. Xia S, Li J, Zu M, Li J, Liu J, Bai X, et al. Small size fullerenol nanoparticles inhibit thrombosis and blood coagulation through inhibiting activities of thrombin and FXa. Nanomedicine: Nanotechnology, Biology, and Medicine. 2018 Apr 1;14(3):929–39.

CHAPTER 5

CONCLUSIONS AND FUTURE WORK

5.1 Conclusions

Titanium surfaces were modified to form nanotubular structures on them using selective anodization. The surfaces were then treated with PEG and Silane to form superhydrophilic and superhydrophobic surfaces respectively. The results from studying the contact angles for the different surfaces indicated a trend of NT-S>Ti-S>Ti>NT-PEG>Ti-PEG>NT and the contact angle values were all statistically different from each other. The surface morphology was observed using SEM which indicated that the surface modifying coatings were very thin and not physically observable. XPS results further consolidate this observation by calculating the thickness of the coatings using the presence of Ti2p on the surface before and after modification. XPS also indicates the presence of Fluorine in Silane modifications which was different from the XPS results of all other surfaces. A dynamic flow chamber was developed to mimic the flow of blood in different parts of the body and to compare the results with static results. All the surfaces were exposed to blood clotting factors like protein adsorption, cell adhesion and activation of platelets both in static and dynamic conditions. The results from protein adsorption indicated that the surfaces modified with silane showed lower protein adsorption rates for both albumin and fibrinogen in static as well as dynamic conditions. Dynamic protein adsorption was similar to static results although the hydrophobic samples showed much lesser adsorption rates compared to the static study. The results of Fibrinogen indicated NT-S was the surface that adsorbed the least protein followed by Ti-S. The cell adhesion results indicated that in general, the surfaces with nanostructures showed lower cell adhesion than titanium. NT-S showed the least adhesion among all surfaces followed by NT. The SEM results followed up on the other results. Platelet activation was analysed after both static and dynamic platelet exposure and none of the observations showed any sign of platelet activation. All of the results indicated NT-S to be the most hemocompatible amongst all

the surfaces. The difference in results in static and dynamic conditions indicate that blood compatibility study need to be investigated in both conditions to obtain a set of results which is representative of blood flow within the entire body.

5.2 Future Work

The future scope of study include increasing the exposure time for dynamic studies to days and possibly generate a model to predict future behaviour for the materials. Even further, PRP which is are used for static and dynamic studies could be inspected using protein assays. Using different flow chambers could also be a way forward that cover different aspects blood thrombus formation and eventual clotting. In this study PRP was flowed in dynamic studies for a limited time and was used for incubation in static for 2 hours but in the future the incubation and the flow time could be extended to various prolonged periods like hours, days, etc. Using the prolonged period we can ideally if used as an implant. Different protein assays can be used to account for the total number of activated platelets which are not getting stuck to the surfaces during static or dynamic testing but might further activate platelets in flow through the chamber or while being reused for another run. P-selectin assay might be a way to analyse the percentage of already activated platelets before starting a testing procedure to know if it is the surface that is not hemocompatible or if it is dealing with already activated platelets to begin with, which will not justify its performance even if the surface is hemocompatible. Other assays that could be performed are platelet Factor IV, complement activation, contact activation etc. Another possible future path would be to try different flow chambers. Instead of syringes used in our study, a peristaltic pump could be used to regulate the flow of PRP or whole blood. Again, a completely new chamber comprising of a chandler loop might be used. A chandler loop uses looped pipes with the materials placed in them. Partially filling the loops with PRP or whole blood and spinning them together using a motor setup and a water bath for temperature control might be an effective way to test multiple samples at the same time.